

**Kinematic Evidence for Top Quark Pair Production in
 $W +$ Multijet Events in $p\bar{p}$ Collisions at $\sqrt{s} = 1.8$ TeV**

F. Abe,¹³ M. G. Albrow,⁷ S. R. Amendolia,²³ D. Amidei,¹⁶ J. Antos,²⁸ C. Anway-Wiese,⁴
 G. Apollinari,²⁶ H. Areti,⁷ M. Atac,⁷ P. Auchincloss,²⁵ F. Azfar,²¹ P. Azzi,²⁰
 N. Bacchetta,¹⁸ W. Badgett,¹⁶ M. W. Bailey,¹⁸ J. Bao,³⁵ P. de Barbaro,²⁵
 A. Barbaro-Galtieri,¹⁴ V. E. Barnes,²⁴ B. A. Barnett,¹² P. Bartalini,²³ G. Bauer,¹⁵
 T. Baumann,⁹ F. Bedeschi,²³ S. Behrends,³ S. Belforte,²³ G. Bellettini,²³ J. Bellinger,³⁴
 D. Benjamin,³¹ J. Benlloch,¹⁵ J. Bensinger,³ D. Benton,²¹ A. Beretvas,⁷ J. P. Berge,⁷
 S. Bertolucci,⁸ A. Bhatti,²⁶ K. Biery,¹¹ M. Binkley,⁷ F. Bird,²⁹ D. Bisello,²⁰ R. E. Blair,¹
 C. Blocker,³ A. Bodek,²⁵ W. Bokhari,¹⁵ V. Bolognesi,²³ D. Bortoletto,²⁴ C. Boswell,¹²
 T. Boulos,¹⁴ G. Brandenburg,⁹ C. Bromberg,¹⁷ E. Buckley-Geer,⁷ H. S. Budd,²⁵
 K. Burkett,¹⁶ G. Busetto,²⁰ A. Byon-Wagner,⁷ K. L. Byrum,¹ J. Cammerata,¹²
 C. Campagnari,⁷ M. Campbell,¹⁶ A. Caner,⁷ W. Carithers,¹⁴ D. Carlsmith,³⁴ A. Castro,²⁰
 Y. Cen,²¹ F. Cervelli,²³ H. Y. Chao,²⁸ J. Chapman,¹⁶ M.-T. Cheng,²⁸ G. Chiarelli,⁸
 T. Chikamatsu,³² C. N. Chiou,²⁸ S. Cihangir,⁷ A. G. Clark,²³ M. Cobal,²³ M. Contreras,⁵
 J. Conway,²⁷ J. Cooper,⁷ M. Cordelli,⁸ C. Couyoumtzelis,²³ D. Crane,¹
 J. D. Cunningham,³ T. Daniels,¹⁵ F. DeJongh,⁷ S. Delchamps,⁷ S. Dell'Agnello,²³
 M. Dell'Orso,²³ L. Demortier,²⁶ B. Denby,²³ M. Deninno,² P. F. Derwent,¹⁶ T. Devlin,²⁷
 M. Dickson,²⁵ J. R. Dittmann,⁶ S. Donati,²³ R. B. Drucker,¹⁴ A. Dunn,¹⁶ K. Einsweiler,¹⁴
 J. E. Elias,⁷ R. Ely,¹⁴ E. Engels, Jr.,²² S. Eno,⁵ D. Errede,¹⁰ S. Errede,¹⁰ Q. Fan,²⁵
 B. Farhat,¹⁵ I. Fiori,² B. Flaughner,⁷ G. W. Foster,⁷ M. Franklin,⁹ M. Frautschi,¹⁸
 J. Freeman,⁷ J. Friedman,¹⁵ H. Frisch,⁵ A. Fry,²⁹ T. A. Fuess,¹ Y. Fukui,¹³ S. Funaki,³²
 G. Gagliardi,²³ S. Galeotti,²³ M. Gallinaro,²⁰ A. F. Garfinkel,²⁴ S. Geer,⁷ D. W. Gerdes,¹⁶
 P. Giannetti,²³ P. Giromini,⁸ L. Gladney,²¹ D. Glenzinski,¹² M. Gold,¹⁸ J. Gonzalez,²¹
 A. Gordon,⁹ A. T. Goshaw,⁶ K. Goulios,²⁶ H. Grassmann,⁶ A. Grewal,²¹ G. Grieco,²³

L. Groer,²⁷ C. Grosso-Pilcher,⁵ C. Haber,¹⁴ S. R. Hahn,⁷ R. Hamilton,⁹ R. Handler,³⁴
 R. M. Hans,³⁵ K. Hara,³² B. Harral,²¹ R. M. Harris,⁷ S. A. Hauger,⁶ J. Hauser,⁴
 C. Hawk,²⁷ J. Heinrich,²¹ D. Cronin-Hennessy,⁶ R. Hollebeek,²¹ L. Holloway,¹⁰
 A. Hölscher,¹¹ S. Hong,¹⁶ G. Houk,²¹ P. Hu,²² B. T. Huffman,²² R. Hughes,²⁵ P. Hurst,⁹
 J. Huston,¹⁷ J. Huth,⁹ J. Hylen,⁷ M. Incagli,²³ J. Incandela,⁷ H. Iso,³² H. Jensen,⁷
 C. P. Jessop,⁹ U. Joshi,⁷ R. W. Kadel,¹⁴ E. Kajfasz,^{7a} T. Kamon,³⁰ T. Kaneko,³²
 D. A. Kardelis,¹⁰ H. Kasha,³⁵ Y. Kato,¹⁹ L. Keeble,⁸ R. D. Kennedy,²⁷ R. Kephart,⁷
 P. Kesten,¹⁴ D. Kestenbaum,⁹ R. M. Keup,¹⁰ H. Keutelian,⁷ F. Keyvan,⁴ D. H. Kim,⁷
 H. S. Kim,¹¹ S. B. Kim,¹⁶ S. H. Kim,³² Y. K. Kim,¹⁴ L. Kirsch,³ P. Koehn,²⁵ K. Kondo,³²
 J. Konigsberg,⁹ S. Kopp,⁵ K. Kordas,¹¹ W. Koska,⁷ E. Kovacs,^{7a} W. Kowald,⁶
 M. Krasberg,¹⁶ J. Kroll,⁷ M. Kruse,²⁴ S. E. Kuhlmann,¹ E. Kuns,²⁷ A. T. Laasanen,²⁴
 N. Labanca,²³ S. Lammel,⁴ J. I. Lamoureux,³ T. LeCompte,¹⁰ S. Leone,²³ J. D. Lewis,⁷
 P. Limon,⁷ M. Lindgren,⁴ T. M. Liss,¹⁰ N. Lockyer,²¹ C. Loomis,²⁷ O. Long,²¹
 M. Loreti,²⁰ E. H. Low,²¹ J. Lu,³⁰ D. Lucchesi,²³ C. B. Luchini,¹⁰ P. Lukens,⁷ J. Lys,¹⁴
 P. Maas,³⁴ K. Maeshima,⁷ A. Maghakian,²⁶ P. Maksimovic,¹⁵ M. Mangano,²³
 J. Mansour,¹⁷ M. Mariotti,²³ J. P. Marriner,⁷ A. Martin,¹⁰ J. A. J. Matthews,¹⁸
 R. Mattingly,¹⁵ P. McIntyre,³⁰ P. Melese,²⁶ A. Menzione,²³ E. Meschi,²³ G. Michail,⁹
 S. Mikamo,¹³ M. Miller,⁵ R. Miller,¹⁷ T. Mimashi,³² S. Miscetti,⁸ M. Mishina,¹³
 H. Mitsushio,³² S. Miyashita,³² Y. Morita,¹³ S. Moulding,²⁶ J. Mueller,²⁷ A. Mukherjee,⁷
 T. Muller,⁴ P. Musgrave,¹¹ L. F. Nakae,²⁹ I. Nakano,³² C. Nelson,⁷ D. Neuberger,⁴
 C. Newman-Holmes,⁷ L. Nodulman,¹ S. Ogawa,³² S. H. Oh,⁶ K. E. Ohl,³⁵ R. Oishi,³²
 T. Okusawa,¹⁹ C. Pagliarone,²³ R. Paoletti,²³ V. Papadimitriou,³¹ S. Park,⁷ J. Patrick,⁷
 G. Pauletta,²³ M. Paulini,¹⁴ L. Pescara,²⁰ M. D. Peters,¹⁴ T. J. Phillips,⁶ G. Piacentino,²
 M. Pillai,²⁵ R. Plunkett,⁷ L. Pondrom,³⁴ N. Produit,¹⁴ J. Proudfoot,¹ F. Ptohos,⁹
 G. Punzi,²³ K. Ragan,¹¹ F. Rimondi,² L. Ristori,²³ M. Roach-Bellino,³³ W. J. Robertson,⁶
 T. Rodrigo,⁷ J. Romano,⁵ L. Rosenson,¹⁵ W. K. Sakumoto,²⁵ D. Saltzberg,⁵
 V. Scarpine,³⁰ A. Schindler,¹⁴ P. Schlabach,⁹ E. E. Schmidt,⁷ M. P. Schmidt,³⁵
 O. Schneider,¹⁴ G. F. Sciacca,²³ A. Scribano,²³ S. Segler,⁷ S. Seidel,¹⁸ Y. Seiya,³²

G. Sganos,¹¹ A. Sgolacchia,² M. Shapiro,¹⁴ N. M. Shaw,²⁴ Q. Shen,²⁴ P. F. Shepard,²²
M. Shimojima,³² M. Shochet,⁵ J. Siegrist,²⁹ A. Sill,³¹ P. Sinervo,¹¹ P. Singh,²² J. Skarha,¹²
D. A. Smith,²³ F. D. Snider,¹² L. Song,⁷ T. Song,¹⁶ J. Spalding,⁷ L. Spiegel,⁷ P. Sphicas,¹⁵
A. Spies,¹² L. Stanco,²⁰ J. Steele,³⁴ A. Stefanini,²³ K. Strahl,¹¹ J. Strait,⁷ D. Stuart,⁷
G. Sullivan,⁵ K. Sumorok,¹⁵ R. L. Swartz, Jr.,¹⁰ T. Takahashi,¹⁹ K. Takikawa,³²
F. Tartarelli,²³ W. Taylor,¹¹ P. K. Teng,²⁸ Y. Teramoto,¹⁹ S. Tether,¹⁵ D. Theriot,⁷
J. Thomas,²⁹ T. L. Thomas,¹⁸ R. Thun,¹⁶ P. Tipton,²⁵ A. Titov,²⁶ S. Tkaczyk,⁷
K. Tollefson,²⁵ A. Tollestrup,⁷ J. Tonnison,²⁴ J. F. de Troconiz,⁹ J. Tseng,¹²
M. Turcotte,²⁹ N. Turini,² N. Uemura,³² F. Ukegawa,²¹ G. Unal,²¹ S. van den Brink,²²
S. Vejcik, III,¹⁶ R. Vidal,⁷ M. Vondracek,¹⁰ R. G. Wagner,¹ R. L. Wagner,⁷ N. Wainer,⁷
R. C. Walker,²⁵ C. H. Wang,²⁸ G. Wang,²³ J. Wang,⁵ M. J. Wang,²⁸ Q. F. Wang,²⁶
A. Warburton,¹¹ G. Watts,²⁵ T. Watts,²⁷ R. Webb,³⁰ C. Wendt,³⁴ H. Wenzel,¹⁴
W. C. Wester, III,¹⁴ T. Westhusing,¹⁰ A. B. Wicklund,¹ E. Wicklund,⁷ R. Wilkinson,²¹
H. H. Williams,²¹ P. Wilson,⁵ B. L. Winer,²⁵ J. Wolinski,³⁰ D. Y. Wu,¹⁶ X. Wu,²³
J. Wyss,²⁰ A. Yagil,⁷ W. Yao,¹⁴ K. Yasuoka,³² Y. Ye,¹¹ G. P. Yeh,⁷ P. Yeh,²⁸ M. Yin,⁶
T. Yoshida,¹⁹ D. Yovanovitch,⁷ I. Yu,³⁵ J. C. Yun,⁷ A. Zanetti,²³ F. Zetti,²³ L. Zhang,³⁴
S. Zhang,¹⁶ W. Zhang,²¹ and S. Zucchelli²

(CDF Collaboration)

¹ *Argonne National Laboratory, Argonne, Illinois 60439*

² *Istituto Nazionale di Fisica Nucleare, University of Bologna, I-40126 Bologna, Italy*

³ *Brandeis University, Waltham, Massachusetts 02254*

⁴ *University of California at Los Angeles, Los Angeles, California 90024*

⁵ *University of Chicago, Chicago, Illinois 60637*

⁶ *Duke University, Durham, North Carolina 27708*

⁷ *Fermi National Accelerator Laboratory, Batavia, Illinois 60510*

⁸ *Laboratori Nazionali di Frascati, Istituto Nazionale di Fisica Nucleare, I-00044 Frascati, Italy*

⁹ *Harvard University, Cambridge, Massachusetts 02138*

- ¹⁰ *University of Illinois, Urbana, Illinois 61801*
- ¹¹ *Institute of Particle Physics, McGill University, Montreal H3A 2T8, and University of Toronto,
Toronto M5S 1A7, Canada*
- ¹² *The Johns Hopkins University, Baltimore, Maryland 21218*
- ¹³ *National Laboratory for High Energy Physics (KEK), Tsukuba, Ibaraki 305, Japan*
- ¹⁴ *Lawrence Berkeley Laboratory, Berkeley, California 94720*
- ¹⁵ *Massachusetts Institute of Technology, Cambridge, Massachusetts 02139*
- ¹⁶ *University of Michigan, Ann Arbor, Michigan 48109*
- ¹⁷ *Michigan State University, East Lansing, Michigan 48824*
- ¹⁸ *University of New Mexico, Albuquerque, New Mexico 87131*
- ¹⁹ *Osaka City University, Osaka 588, Japan*
- ²⁰ *Università di Padova, Istituto Nazionale di Fisica Nucleare, Sezione di Padova, I-35131 Padova, Italy*
- ²¹ *University of Pennsylvania, Philadelphia, Pennsylvania 19104*
- ²² *University of Pittsburgh, Pittsburgh, Pennsylvania 15260*
- ²³ *Istituto Nazionale di Fisica Nucleare, University and Scuola Normale Superiore of Pisa, I-56100 Pisa, Italy*
- ²⁴ *Purdue University, West Lafayette, Indiana 47907*
- ²⁵ *University of Rochester, Rochester, New York 14627*
- ²⁶ *Rockefeller University, New York, New York 10021*
- ²⁷ *Rutgers University, Piscataway, New Jersey 08854*
- ²⁸ *Academia Sinica, Taiwan 11529, Republic of China*
- ²⁹ *Superconducting Super Collider Laboratory, Dallas, Texas 75237*
- ³⁰ *Texas A&M University, College Station, Texas 77843*
- ³¹ *Texas Tech University, Lubbock, Texas 79409*
- ³² *University of Tsukuba, Tsukuba, Ibaraki 305, Japan*
- ³³ *Tufts University, Medford, Massachusetts 02155*
- ³⁴ *University of Wisconsin, Madison, Wisconsin 53706*
- ³⁵ *Yale University, New Haven, Connecticut 06511*

Abstract

We present a study of W +multijet events that compares the kinematics of the observed events with expectations from direct QCD W +jet production and from production and decay of top quark pairs. The data were collected in the 1992-93 run with the Collider Detector at Fermilab (CDF) from 19.3 pb^{-1} of proton-antiproton collisions at $\sqrt{s} = 1.8 \text{ TeV}$. A $W + \geq 2$ jet sample and a $W + \geq 3$ jet sample are selected with the requirement that at least the two or three jets have energy transverse with respect to the beam axis in excess of 20 GeV. The jet energy distributions for the $W + \geq 2$ jet sample agree well with the predictions of direct QCD W production. From the $W + \geq 3$ jet events, a “signal sample” with an improved ratio of $t\bar{t}$ to QCD produced W events is selected by requiring each jet to be emitted centrally in the event center of mass frame. This sample contains 14 events with unusually hard jet E_T distributions not well described by expectations for jets from direct QCD W production and other background processes. Using expected jet E_T distributions, a relative likelihood is defined and used to determine if an event is more consistent with the decay of $t\bar{t}$ pairs, with $M_{top} = 170 \text{ GeV}/c^2$, than with direct QCD W production. Eight of the 14 signal sample events are found to be more consistent with top than direct QCD W production, while only 1.7 such top-like events are expected in the absence of $t\bar{t}$. The probability that the observation is due to an upward fluctuation of the number of background events is found to be 0.8%. The robustness of the result was tested by varying the cuts defining the signal sample, and the largest probability for such a fluctuation found was 1.9%. Good agreement in the jet spectra is obtained if jet production from $t\bar{t}$ pair decays is included. For those events kinematically more consistent with $t\bar{t}$ we find evidence for a b -quark content in their jets to the extent expected from top decay, and larger than expected for background processes. For events with four or more jets, the discrepancy with the predicted jet energy distributions from direct QCD W production, and the associated excess of b -quark content is more pronounced.

PACS numbers: 14.80.Dq, 13.85.Qk, 13.85.Ni

1 Introduction

Recently CDF presented evidence for top quark pair production, both via the observation of events with two high P_T leptons and via the observation of events with a W , 3 or more jets, and a jet tagged as a b quark [1]. In that analysis the distributions of specific *kinematic* parameters of the events, such as jet energies and angles, were not used to discriminate between signal and background. It is of interest to search for evidence of top quark pair production based on this event structure and to determine whether one can select a top quark enriched sample of events with suitable cuts on kinematic variables.

The main background to $t\bar{t}$ production comes from higher order QCD production of quarks and gluons in association with direct W production. Recent experiments have indicated that the top quark mass is larger than of order $130 \text{ GeV}/c^2$ [1] [2] [3]. For such a heavy top quark it is difficult to distinguish the signal from the background based on the properties of the W . However, the jets in $t\bar{t}$ events have higher energies on average than those accompanying the W in direct W production, and are expected to be produced at larger angles relative to the beam direction. In this paper we separate $t\bar{t}$ events where one of the W 's decays leptonically and the other hadronically ($t\bar{t} \rightarrow W^+b + W^- \bar{b} \rightarrow l\nu b + q\bar{q}\bar{b}$) by exploiting these properties.

The paper is organized as follows. Section 2 describes the analysis cuts used to define the W +jet sample. Section 3 gives a brief comparison of the kinematics of directly produced W +jet events and of W +jet events from top quark decay, and explains the analysis strategy. Section 4 summarizes various comparisons of QCD Monte Carlo predictions which successfully fit experimental measurements in processes where a top quark contribution can be neglected. Kinematic features of our W + ≥ 3 jet data sample are compared to background and to top quark prediction in Section 5. This comparison shows evidence for a top quark-like component in the data. Section 6 combines this result with the independent information obtained from the algorithms which provide identification of b quarks in the events. In Section 7, as an additional test, we look for an excess of W +4 jet events in the top quark candidate sample. The conclusions are presented in Section 8.

2 Data Selection

This analysis is based on 19.3 pb^{-1} of data from 1.8 TeV $p\bar{p}$ collisions taken with the CDF detector during the 1992-1993 Tevatron run. The CDF detector is described in detail elsewhere [1],[4],[5]. For this run, the tracking system was upgraded with a high precision silicon vertex detector (SVX) [5], and the muon detector was improved at pseudorapidity [6] $|\eta| < 0.6$ by adding an absorber of 0.6 m of steel followed by drift chambers. In addition, the coverage of the central muon detector was extended to the region of pseudorapidity $0.6 < |\eta| < 1.0$ (over about 2/3 of the azimuth) with drift chambers and scintillation counters. The transverse momentum P_T , defined as $P_T = P \sin \theta$, is the projection of the observed momentum (P) onto the plane transverse to the beam axis. Similarly, the transverse energy is defined as: $E_T = E \sin \theta$, where E is the energy measured in the calorimeter. The identification and measurement of isolated, high- P_T electrons and muons, the measurement of the missing E_T (\cancel{E}_T) indicative of neutrinos in the events, the jet clustering algorithm, and the jet energy corrections are discussed in Ref. [1],[7] and [8].

A sample of $W \rightarrow e\nu(\mu\nu)$ candidate events was selected with the requirement that $E_T^e > 20 \text{ GeV}$ ($P_T^\mu > 20 \text{ GeV}/c$) and $\cancel{E}_T > 25 \text{ GeV}$. In addition, the transverse mass, defined as $M_T = [2E_T\cancel{E}_T(1-\cos\Delta\phi)]^{1/2}$ (where $\Delta\phi$ is the difference in azimuthal angle between the missing energy direction and the lepton), was required to be larger than $40 \text{ GeV}/c^2$. The jets are reconstructed with a cone size $R = \sqrt{\Delta\Phi^2 + \Delta\eta^2} = 0.4$ (where $\Delta\Phi$ is the cone half-width in azimuth and $\Delta\eta$ is the cone half-width in pseudorapidity). The jet energies are corrected by a rapidity and energy dependent factor which accounts for calorimeter non-linearity and reduced response at detector boundaries [7], [8]. In addition to these detector effects, a correction is also made for energy which is radiated out of the jet reconstruction cone. The \cancel{E}_T is calculated after correcting the jet energies. In order to allow for a clean separation of jets from each other and to facilitate the comparison of energy distributions with theoretical expectations, the centroids of the three leading jets are required to be separated from each other by $\Delta R \geq 0.7$.

Backgrounds from Z decay, Drell Yan production of dileptons, and possible $t\bar{t}$ events

in which both W 's decay leptonically are removed by rejecting events with an additional isolated track with $P_T > 15$ GeV/ c in the central tracking system that is not associated with the primary lepton. Tracks are defined as isolated when the total transverse momentum of the charged tracks (other than the track in question) in a cone of radius $R = 0.4$ centered on the track is less than 0.1 times the P_T of the track. A study of a QCD multijet sample has shown that fewer than 1% of jets with $E_T(\text{jet}) > 20$ GeV are rejected by this cut [9]. An additional Z removal algorithm eliminates events with an oppositely-charged dilepton (ee or $\mu\mu$) invariant mass in the range 70 to 110 GeV/ c^2 .

A sample of $W + \geq 2$ jets with the two leading jets having $E_T(\text{jet}) > 20$ GeV and $|\eta(\text{jet})| < 2$ is selected, where the $t\bar{t}$ contribution is expected to be relatively small. This sample is studied in order to check whether the energy spectra of the leading jets agree with QCD prediction for direct $W + \text{jet}$ production. The search for a $t\bar{t}$ component is performed in the subsample with ≥ 3 such jets.

The primary differences in event selection between this analysis and the analysis of $W + \geq 3$ jets performed in Ref. [1] are that (1) corrections to jet energy and \cancel{E}_T are made *prior* to event selection, (2) the jets are explicitly required to be separated by $\Delta R > 0.7$, (3) a cut is added on the transverse mass, and (4) the rejection of events with an additional isolated track is included. These changes are made to simplify the comparison of observed jet energies with theoretical predictions for direct $W + \text{jet}$ production and to reduce background from non- W sources.

The fraction of all $t\bar{t}$ events that should fall into our $W + \geq 3$ jet sample is determined from the HERWIG $p\bar{p} \rightarrow t\bar{t}$ Monte Carlo program and the CDF detector simulation. Corrections to the acceptance for trigger inefficiencies and differences in lepton identification between data and Monte Carlo simulation are identical to those described in Ref. [1]. For this analysis we find that the top quark acceptance ranges from $2.7 \pm 0.2\%$ at $M_{top} = 150$ GeV/ c^2 to $3.0 \pm 0.2\%$ at $M_{top} = 190$ GeV/ c^2 . The number of $t\bar{t}$ events expected in the $W + \geq 3$ jet sample using the Standard Model top quark production cross section from Ref. [10] is about 7 for $M_{top} = 170$ GeV/ c^2 . Using the cross section from Ref. [1] we expect $16.7^{+7.6}_{-6.0}$

events. We observe a total of 49 events, 25 of them being in common with the 52 $W + \geq 3$ jet event sample of Ref. [1]. For top quark events the two sets of cuts make little difference: about 90% of all top quark events contained in the sample of 49 events will also show up in the sample of 52. QCD $W +$ jet events often will be close to the jet E_T cuts. Therefore only approximately 67% of QCD events from the sample of 49 will also be found under the cuts of the sample of 52. If we assume that all 49 events are from QCD, then we expect an overlap of approximately 33 events to be compared to the observed overlap of 25 events.

3 W and $t\bar{t}$ Kinematics

Monte Carlo event samples are used to compare the distribution of several kinematic variables for top quark and background events. Samples of top quark events of various masses were generated with both ISAJET [11] and HERWIG [12], and it was verified that both Monte Carlo generators give similar results. $W +$ jet events were generated according to the lowest order matrix elements for the production of a W with n final state partons. The complete sets of matrix elements at tree level have been determined for $n = 0, 1, 2, 3, 4$ and are implemented in the program VECBOS [13]. To avoid infrared divergences which would occur at small angles and small P_T , cuts are applied in the event generation that require $P_T(\text{parton}) > 10 \text{ GeV}/c$, $|\eta(\text{parton})| < 3.5$, and $\Delta R(\text{parton-parton}) > 0.4$. Unless otherwise noted, $Q^2 = M_W^2$ has been used for the α_s scale and the structure functions; this choice yields the hardest jet energy spectrum of a number of Q^2 scales considered. Two different techniques are used to transform the partons produced by VECBOS into hadrons and jets, which can then be processed through the CDF detector simulation. One method employs a Field and Feynman fragmentation function [14] (“SETPRT”), tuned to reproduce the features of observed inclusive QCD jets. The other (“HERPRT” [15]) uses part of the QCD shower evolution Monte Carlo HERWIG. In this case the events generated by VECBOS are assigned an appropriate flavour and colour configuration, and are processed through the HERPRT initial and final state evolution program. Unless otherwise noted, the results presented here will use the HERWIG approach. The Monte Carlo events have then been

processed through a full simulation of the CDF detector and reconstructed in the same manner as the data.

The choice of suitable kinematic parameters to distinguish top quark events from background is presently the subject of considerable work. The D0 collaboration has used event aplanarity and the scalar sum of the jet transverse energies [2]. CDF has studied these variables as well as other parameters involving combinations of jet energies and angles [16]. Work is presently in progress to identify which parameters provide optimal information. In this study we have focused the analysis on jet transverse energies and polar angles. Our studies have indicated that these variables are among the most powerful at separating top quark signal from direct W + jet background.

Jets are ordered in E_T with jet₁ having the highest energy, E_{T1} . It was found that the E_{T2} or E_{T3} variables are better discriminant between QCD background and top quark events than E_{T1} . A qualitative indication of the separation that can be obtained between $t\bar{t}$ and direct W + jet production on the basis of E_{T2} , E_{T3} is shown in Figure 1, which presents the predicted density $\frac{1}{\sigma}d^2\sigma/dE_{T2}dE_{T3}$ of W + ≥ 3 jet and $t\bar{t}$ events ($M_{top} = 170$ GeV/ c^2). The distributions are different for heavy top quark and background events, with $t\bar{t}$ events characterized by higher E_T jets.

Selection of events based on the presence and energy of a fourth jet is also predicted to be a good discriminant between $t\bar{t}$ and direct W production. However, in this analysis we do not *require* a fourth jet. This is done in order to minimize: (a) uncertainties in the theoretical calculation of the E_{T4} spectrum in $t\bar{t}$ events with accompanying gluon radiation, (b) the uncertainty in the reconstruction efficiency and in the energy measurement of low energy jets. The presence of a fourth jet will later be examined in this paper as an indication of whether top quark is present.

Another variable which can discriminate between W + jets and $t\bar{t}$ is $|\cos\theta^*|$ [17], where θ^* is the angle between a jet and the incident proton direction in the center of mass of the hard subprocess. The component of the hard subprocess center of mass velocity along the beam direction is calculated using the four-momenta of the W and all jets with

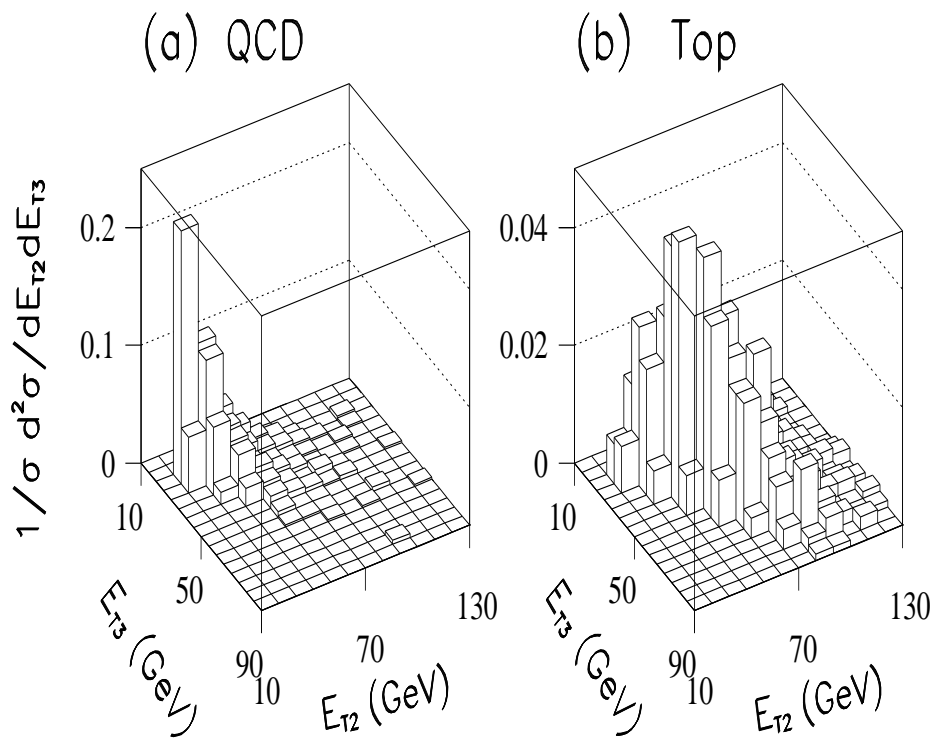


Figure 1: $\frac{1}{\sigma} \frac{d^2\sigma}{dE_{T2}dE_{T3}}$ for (a) QCD $W + 3$ jet and (b) top quark ($M_{top} = 170 \text{ GeV}/c^2$) Monte Carlo events.

$E_T > 15$ GeV. Jets are included down to this relatively low energy in order to reconstruct the laboratory velocity of the initial state subprocess as well as possible. In calculating the W 4-momentum, the longitudinal component of the neutrino cannot be determined unambiguously and for simplicity is taken to be zero. The expected distribution of the jets as a function of $|\cos\theta^*|_{max}$, the maximum of $|\cos\theta^*(jet_i)|$, $i=1,2,3$ is shown in Figure 2(a). The inclusive jet distribution for direct W events is peaked in the forward direction while that for top quark events is more central. As in Ref. [1], jet_1 , jet_2 and jet_3 are required to have $|\eta(jet)| < 2$. The $|\cos\theta^*|$ distribution after this cut is shown in Figure 2(b). After the $|\eta(jet)| < 2$ cut, our studies indicate that a $|\cos\theta^*|$ cut still improves the signal/background ratio. It also allows one to define a background depleted “signal sample” as those events in which each of the three leading jets satisfies $|\cos\theta^*| < 0.7$, and a background enriched “control sample” which contains all events in which at least one of the jets has $|\cos\theta^*| > 0.7$. The Monte Carlo predictions show that the $|\cos\theta^*|$ cut generates a harder jet E_T distribution for top quark production, while for direct $W + jet$ production it leaves the E_T distributions essentially unaffected. Therefore an analysis which attempts to separate top quark from background based on the shape of the E_T distributions can be expected to become more discriminating after applying the $|\cos\theta^*|$ cut.

Using the Standard Model $t\bar{t}$ cross section from Ref. [10] we expect approximately 6 events in the signal sample and 7 in the control sample for a top quark mass of $150 \text{ GeV}/c^2$, while for a top quark mass of $190 \text{ GeV}/c^2$ we expect approximately two events each in the signal and control samples. Assuming the top quark production cross section from Ref. [1], the number of top quark events expected for $M_{top} = 170 \text{ GeV}/c^2$ is $7.7^{+3.5}_{-2.8}$ in the signal sample and $9.0^{+4.1}_{-3.2}$ in the control sample. The signal sample contains 14 events and the control sample 35 events. Therefore in the signal sample a signal/background of the order of 1 can be expected, while in the control sample this ratio would be nearly three times worse.

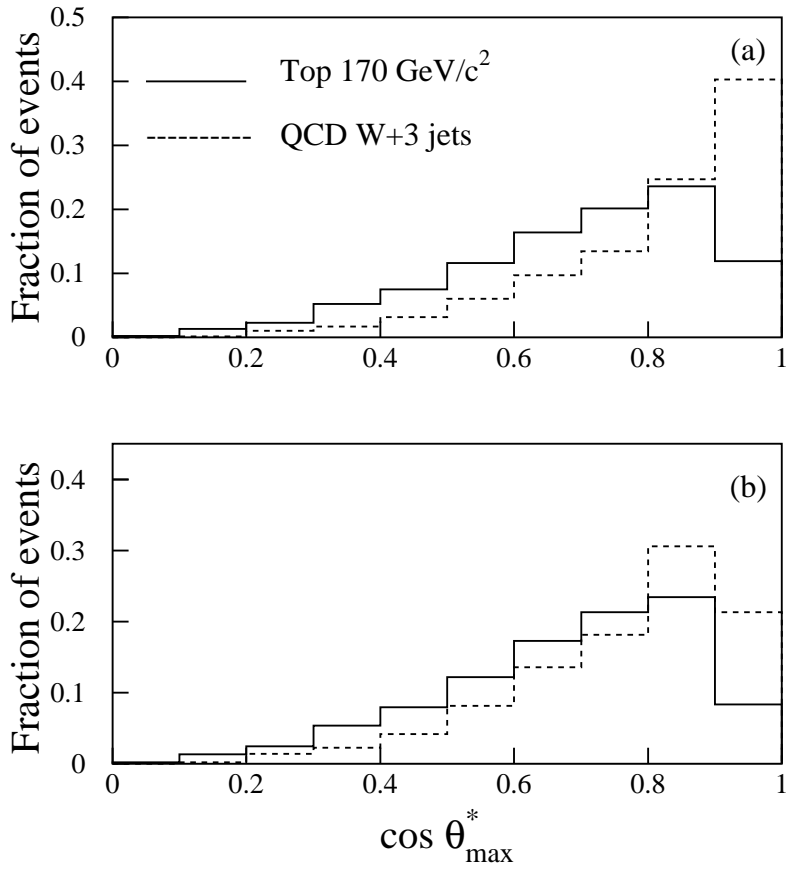


Figure 2: Distributions of the $|\cos \theta_{\max}^*|$ variable predicted by the HERWIG top quark ($M_{\text{top}} = 170 \text{ GeV}/c^2$) and VECBOS $W + 3$ jet calculations for: (a) the inclusive distribution and (b) after applying the cut on $|\eta(\text{jets})| < 2$. The distributions are normalized to unit area.

4 Reliability of $W + \text{Multijet}$ Predictions

In subsequent sections a detailed comparison is made for the observed jet energy distributions for events that contain a W and ≥ 3 jets with the predictions of QCD direct production of W and jets (as implemented in the VECBOS program). It is therefore important to investigate to what extent these predictions are reliable. Previously CDF has compared the cross section for $W + n$ jet production ($n \leq 4$) with QCD predictions [18] and found good agreement. In addition, the jet energy distributions and rapidities for $W + 1$ jet and $W + 2$ jets show good agreement with the QCD calculations [18]. The UA2 collaboration at CERN has examined the transverse energy distributions for multijet events with up to six final state partons and found good agreement [19] with expectations from QCD. CDF has also found excellent agreement between observation and QCD predictions for inclusive distributions in 3 and 4 jet data samples [7][8]. Although the UA2 comparison and the CDF multijet comparison involve a different set of matrix elements than for jets associated to W production, they demonstrate that in terms of jet detection and reconstruction, excellent agreement is obtained between observations and theory for events containing as many as four jets.

A good test is provided by the CDF $W + \geq 2$ jet data sample, which has relatively high statistics, is kinematically similar to the $W + \geq 3$ jet sample, and has a relatively small fractional contribution from top quark.

The angular distributions of data and VECBOS events are compared in Figure 3 in terms of the variable $|\cos \theta^*|_{max}$, which is here the maximum of $|\cos \theta^*(\text{jet}_i)|$, $i=1,2$. As for the $W + \geq 3$ jet sample, a cut on the jet rapidity was applied at $|\eta(\text{jet})| < 2$. The Monte Carlo prediction is normalized to the data. The agreement is excellent. The E_{T1} and E_{T2} distributions of these $W + \geq 2$ jet events are compared to VECBOS predictions in Figure 4 under the requirement that both jets have $|\cos \theta^*| < 0.7$. The Monte Carlo prediction is normalized to the data. The confidence level of the likelihood that the data are consistent with Monte Carlo predictions is 55% for Fig. 4(a) and 69% for Fig. 4(b). While the VECBOS calculation has no phenomenological parameters, the results do depend on the

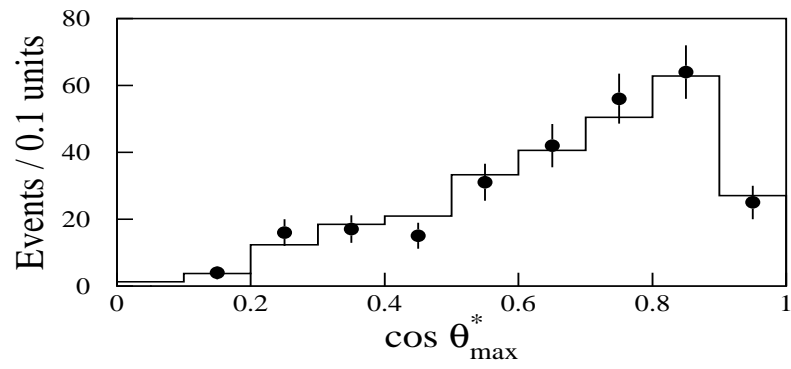


Figure 3: $|\cos \theta^*|_{\max}$ for $W + \geq 2$ jets showing data (points with error bars) and VECBOS $W + 2$ jet events (histogram).

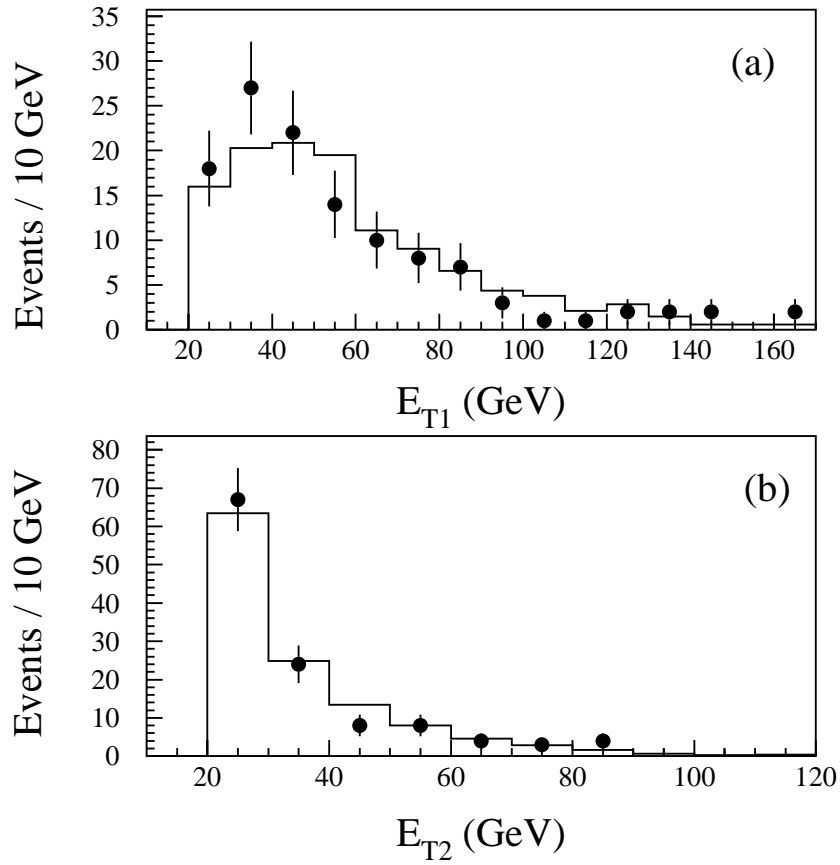


Figure 4: E_T distributions of $W + \geq 2$ jet showing data (points with error bars) and VECBOS $W + 2$ jet events (histograms). (a) leading jet, (b) second to leading jet.

choice of the Q^2 scale and on the minimum separation and P_T of the generated jets. Use of $Q^2 = \langle P_T \rangle^2$ instead of $Q^2 = M_W^2$ yields softer spectra. The agreement between data and predictions is equally good. With the choice $Q^2 = \langle P_T \rangle^2$ the confidence level of the likelihood that the data are consistent with Monte Carlo predictions is 62% for both the E_{T1} and E_{T2} distributions. Since top quark events are expected to give harder jet energy spectra than direct W +jet production, our default choice, $Q^2 = M_W^2$, (see Section 3) is conservative. Additional tests on the sensitivity to the Q^2 scale of $W + \geq 3$ jet Monte Carlo predictions are shown in the next section. Finally, a test of the predictions of jet production associated with vector bosons may be obtained from the $Z + \geq 3$ jets sample, where little contamination from Standard Model top quark events is expected. Data and predictions are shown in Figure 5. While the statistics are limited, the agreement is good. In the higher statistics $Z + \geq 2$ jet sample, one also finds good agreement between data and predictions for the E_T distributions of the two leading jets.

5 Kinematic Analysis

As discussed in Section 3, a signal sample of 14 events is defined by the requirement that the three leading jets have $|\cos\theta^*(\text{jet})| < 0.7$. The background enriched control sample, where at least one jet has $|\cos\theta^*(\text{jet})| > 0.7$ contains 35 events. Figure 6 shows the E_T distributions of the three leading jets in the signal enriched sample. Figure 7 shows the same distributions for the process $W + 3$ jets as predicted by VECBOS and for top quark production modeled with the HERWIG Monte Carlo at a top quark mass of 170 GeV/c². The distributions are normalized to unit area. The E_T distributions of the data are harder than those expected from VECBOS. To combine the information from both E_{T2} and E_{T3} , a discriminating function, “absolute likelihood”, is defined as follows:

$$L_{abs} = \left(\frac{1}{\sigma} \frac{d\sigma}{dE_{T2}} \right) \times \left(\frac{1}{\sigma} \frac{d\sigma}{dE_{T3}} \right) \quad (1)$$

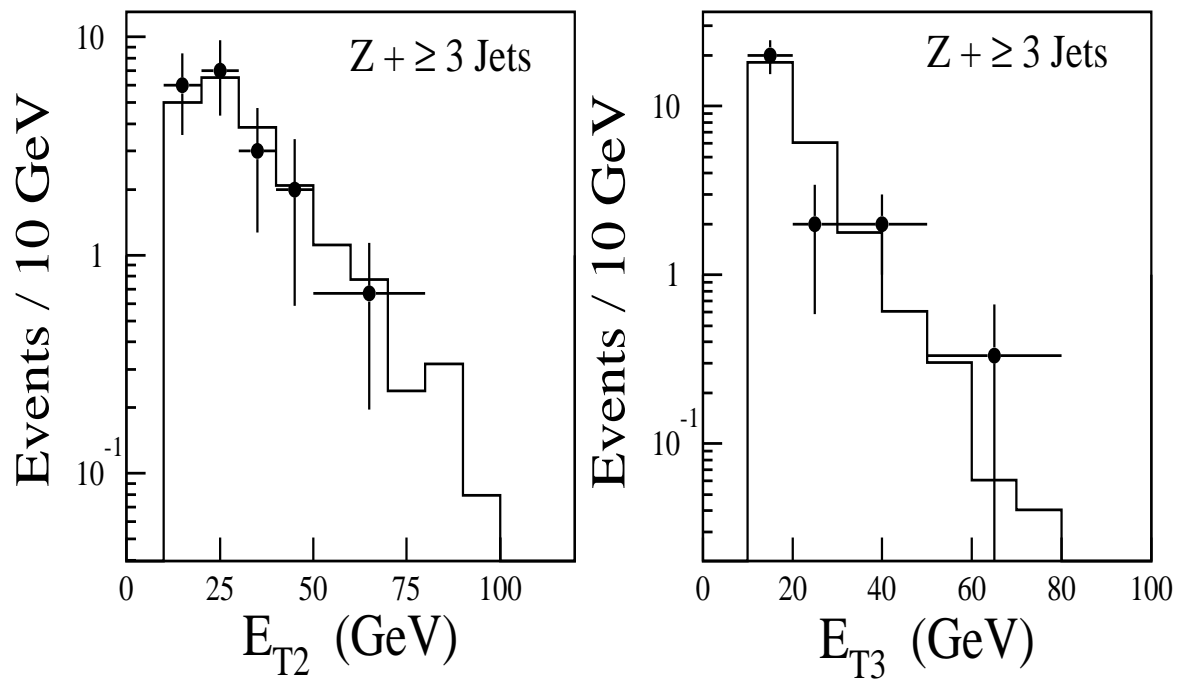


Figure 5: E_T distributions of second and third leading jets in $Z + \geq 3$ jet (inclusive) data (shown as points with error bars) and VECBOS $Z + 3$ jet events (histograms).

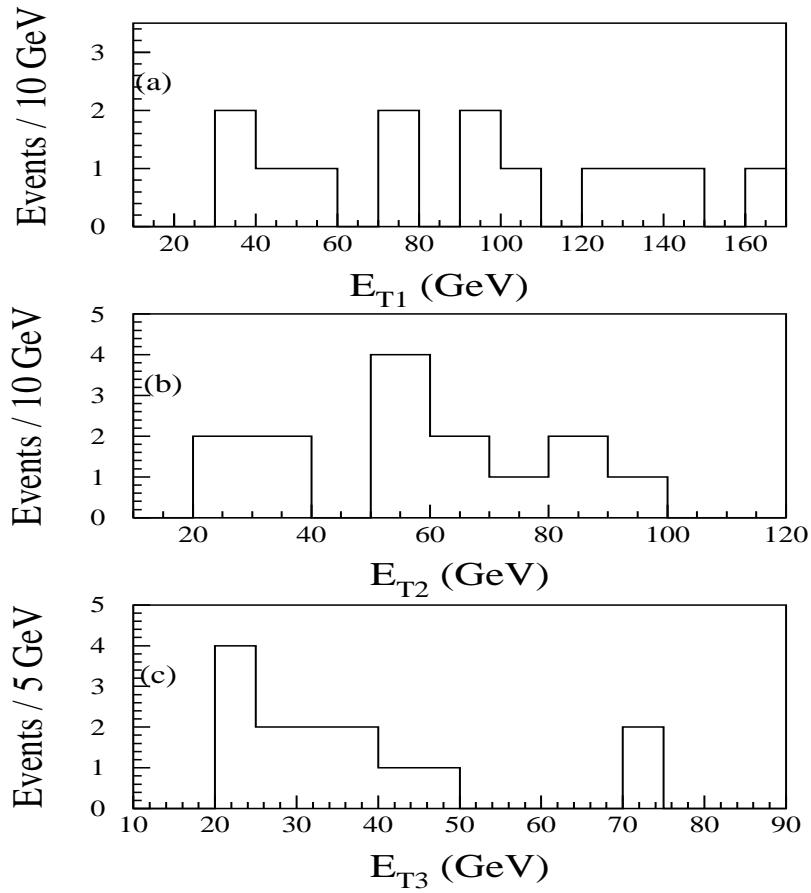


Figure 6: Jet energy distributions for the three leading jets in the 14 events passing the signal sample selection cuts. There is one overflow in E_{T1} at $E_{T1} = 224$ GeV.

Figure 7: Jet energy distributions for HERWIG top quark (solid line) and VECBOS $W + 3$ jet events (dashed line) passing the signal sample selection cuts. Each distribution is normalized to unit area.

that is, as the product of the two differential transverse energy distributions each normalized to unit area. The $\frac{d\sigma}{dE_T}$ are derived from the Monte Carlo simulated distributions fitted by analytical functions. A L_{abs} function can be defined for any process for which a model exists, in particular for QCD $W+ \geq 3$ jets (L_{abs}^{QCD}) and top quark (L_{abs}^{top}). The L_{abs} 's can be combined to define a ‘‘relative likelihood’’ (L_{rel}) for top quark versus QCD as

$$L_{rel} = L_{abs}^{top}/L_{abs}^{QCD}. \quad (2)$$

Note that the absolute likelihoods are not probabilities, since E_{T2} and E_{T3} are correlated. The relative likelihood allows one to compare each individual event to the expectation from QCD and from top quark in terms of a single number. This ‘‘kinematic tag’’ provides a natural definition of the cut which discriminates events which are more top quark-like from events which are more QCD-like. A possible disadvantage of L_{rel} is its dependence on M_{top} . In particular, a L_{rel} which is optimized for a certain top quark mass may have reduced sensitivity if the actual top quark mass is significantly different from the assumed mass. We choose for our analysis $M_{top} = 170$ GeV/ c^2 , based on the results of Ref. [1]. We discuss the effect of a possible different choice in Section 5.1.

5.1 Data–Monte Carlo comparison

Figure 8 shows a comparison of the expected and observed distributions for $\ln(L_{abs}^{QCD})$ for the $W+ \geq 2$ jet and $W+ \geq 3$ jet signal and control samples. In the case of $W+ \geq 2$ jets, the L_{abs} is defined as the product of the E_{T1} and E_{T2} distributions, since a third jet is not always present in the event. The $W+ \geq 2$ jet sample is expected to have a small top quark fraction. The comparison with the VECBOS prediction (Fig. 8(a)) shows good agreement. The $W+ \geq 3$ jet control sample data, where the QCD background is expected to dominate, also agree with the QCD prediction as shown in Figure 8(b). In the $W+ \geq 3$ jet signal sample (Figure 8(c)), where a $t\bar{t}$ contribution could be present, VECBOS predictions and data are somewhat different. In order to check how significant this difference is we performed a likelihood calculation, by assuming a Poisson distribution

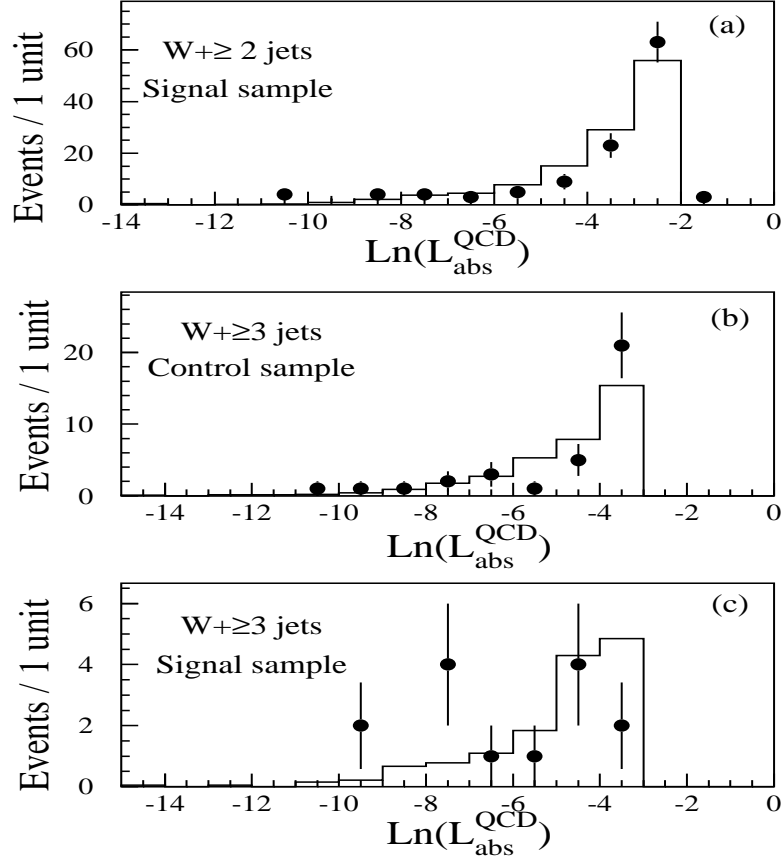


Figure 8: QCD-predicted absolute likelihood distributions (histograms) compared to data (points with error bars). (a): the two leading jets in $W + \geq 2$ jets, a cut $|\cos\theta^*| < 0.7$ was applied to jet_1 and jet_2 ; (b): $\text{jet}_2, \text{jet}_3$ in the control sample; (c) : $\text{jet}_2, \text{jet}_3$ in the signal sample.

with mean equal to the Monte Carlo prediction for each bin. A confidence level of 19.6% is found for VECBOS to agree with the data of Figure 8(b), and 2.7% for Figure 8(c). The likelihood for Figure 8(c) is small enough to suggest a component in the signal sample not well described by VECBOS. The expectations for HERWIG $t\bar{t}$ events, when interpreted as direct $W + \text{jet}$ events, are shown in Figure 9 for a number of different top quark masses. The signal sample data distribution in $\text{Ln}(L_{\text{abs}}^{\text{QCD}})$ seen in Figure 8(c) is consistent with a combination of direct $W + \text{jet}$ events and of $t\bar{t}$ events in a wide mass range around $M_{\text{top}} = 170 \text{ GeV}/c^2$. Figure 10(a) shows how the VECBOS $W + 3$ jet events and HERWIG top quark events are distributed in relative likelihood, $\text{Ln}(L_{\text{rel}}^{t170})$, when the cuts of the signal

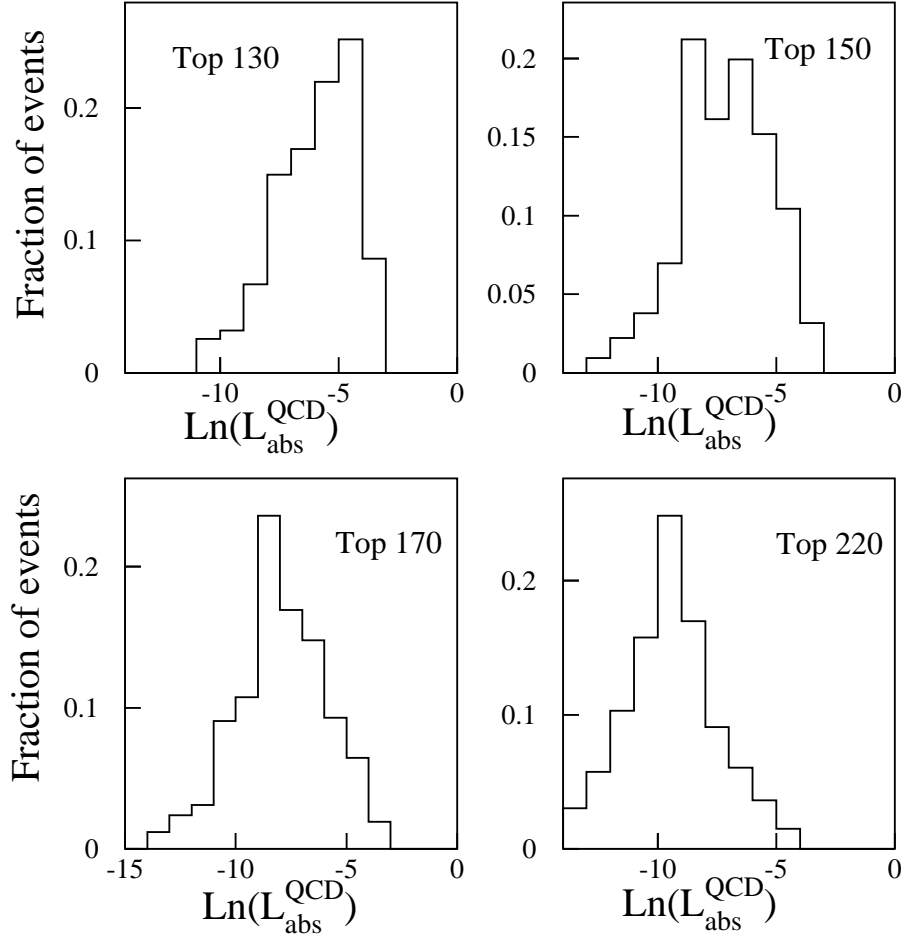


Figure 9: Expected distributions of $t\bar{t}$ Monte Carlo (HERWIG) events as a function of $\ln(L_{\text{abs}}^{\text{QCD}})$, when interpreted as direct W + jet events. The distributions are normalized to unit area.

sample are applied. The symbol L_{rel}^{t170} indicates that $M_{top} = 170 \text{ GeV}/c^2$ was used to predict the expected E_{T2} and E_{T3} distributions. The two distributions are separated well enough to make a top quark signal visible, provided the signal/background is of order 1 as argued in Section 3. Figure 10(b) shows how the data events of the signal sample are distributed in $\ln(L_{rel}^{t170})$, along with the VECBOS distribution from Figure 10(a), normalized to the data at $\ln(L_{rel}^{t170}) < 0$. The data are not distributed as expected from a pure QCD W +jet sample, and look like a superposition of $t\bar{t}$ and QCD events.

We find 6 events with $\ln(L_{rel}^{t170}) < 0$ (more QCD-like) and 8 events with $\ln(L_{rel}^{t170}) > 0$ (more top quark-like). If we normalize the VECBOS distribution, 78% of which is expected to have $\ln(L_{rel}^{t170}) < 0$, to the 6 events observed in that region, then we expect $1.68_{-0.62}^{+0.85}$ VECBOS events with $\ln(L_{rel}^{t170}) > 0$ compared to 8 events observed. This excess represents kinematic evidence for the presence of $t\bar{t}$ production.

Although $M_{top} = 170 \text{ GeV}/c^2$ was assumed, the result is not sensitive to the precise value of M_{top} . As an example, Figure 11(a) shows the expected distributions in $\ln(L_{rel}^{t150})$ for VECBOS $W + 3$ jets and HERWIG $t\bar{t}$ events if $M_{top} = 150 \text{ GeV}/c^2$ is assumed. The two samples are still well separated. The data are distributed as shown in Figure 11(b), and still indicate a superposition of the two processes. The results of a two-component fit to the $\ln(L_{rel}^{t170})$ distribution as a function of M_{top} and the significance of the observed excess at positive $\ln(L_{rel}^{t170})$ will be examined in a later section.

5.2 Evaluation of the statistical significance

The probability that a background fluctuation can produce the observed excess at $\ln(L_{rel}^{t170}) > 0$ is calculated from the binomial probability that given the 14 signal sample events, they are distributed with 8 or more events in the positive $\ln(L_{rel}^{t170})$ side. The calculation makes use of the fraction of QCD W +jet events expected at $\ln(L_{rel}^{t170}) < 0$ and of the statistical error on the fraction. For the primary result (shown in line 1 of Table 1) VECBOS $W + 3$ parton production with a choice of $Q^2 = M_W^2$ and the HERPRT fragmen-

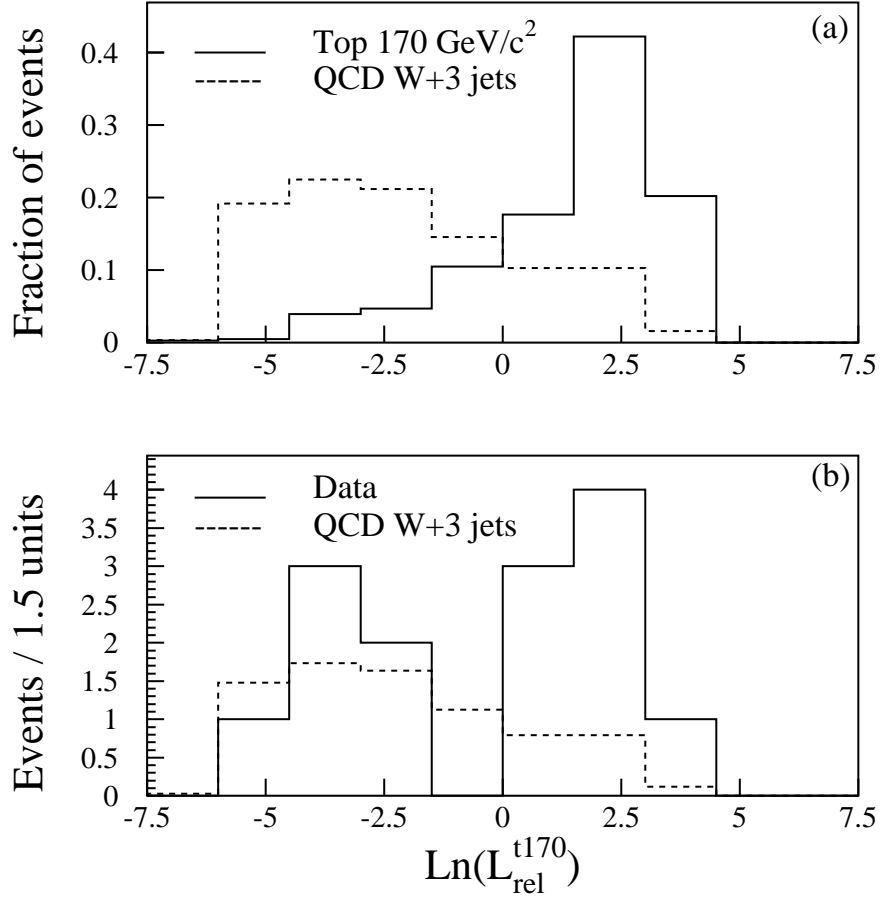


Figure 10: $\text{Ln}(L_{\text{rel}}^{t170})$ for QCD VECBOS, top quark HERWIG ($M_{\text{top}} = 170 \text{ GeV}/c^2$) and data events for $W + 3$ or more central jet events (signal enriched sample). (a): $W + \geq 3$ jet VECBOS (dotted histogram) and top quark HERWIG (solid histogram), normalized to unit area. (b): data (solid histogram) and VECBOS (dotted histogram). VECBOS is normalized to data in the region $\text{Ln}(L_{\text{rel}}^{t170}) < 0$.

Figure 11: (a) Expected distribution in $\ln(L_{rel}^{t150})$ of QCD and $t\bar{t}$ events, for $M_{top} = 150$ GeV/ c^2 ; (b) the data displayed as a function of the same variable. The dotted histogram shows the QCD distribution normalized to the data at $\ln(L_{rel}^{t150}) < 0$.

tation is used. In this case the probability to observe 8 or more events from a background fluctuation is 0.5%. This disagreement between observation and the VECBOS prediction is large enough to suggest the possibility that either VECBOS is wrong, or that there is an additional high E_T process present in the data sample.

Next we address systematic uncertainties in the Monte Carlo predictions. One sys-

	% rate at $\ln(L_{rel}^{t170}) < 0$
1. HERPRT ($Q^2=M_W^2$)	78.2 ± 2.4
2. E_T scaled down	81.2 ± 2.6
3. E_T scaled up	74.9 ± 2.2
4. HERPRT ($Q^2=\langle P_T \rangle^2$)	80.4 ± 5.5
5. SETPRT ($Q^2=\langle P_T \rangle^2$)	81.1 ± 2.8
6. HERPRT ($Q^2=M_W^2$) + Systematics + non- W backgrounds	78 ± 5

Table 1: Fraction of background events at $\ln(L_{rel}^{t170}) < 0$ for different predictions of the $\ln(L_{rel}^{t170})$ shape. The predictions compare to 6 data events observed at $\ln(L_{rel}^{t170}) < 0$ and 8 events at $\ln(L_{rel}^{t170}) > 0$.

tematic uncertainty is the possible difference in the energy scale of data and Monte Carlo events. The relative uncertainty in the jet energy scale of the calorimeter decreases with increasing the jet energy. These effects have been taken into account by varying Monte Carlo jet energies by an uncertainty from $\pm 10\%$ at 8 GeV to $\pm 3\%$ at 100 GeV to account for detector effects, in quadrature with a $\pm 10\%$ uncertainty due to the assignment of energies to partons in the presence of gluon radiation, which is the dominant uncertainty. The second and third lines of Table 1 show the results. The uncertainty in VECBOS due to the lack of higher order contributions can be addressed by changing the Q^2 scale in α_s . For comparison with the results shown in the first line of Table 1, the results for $Q^2=\langle P_T \rangle^2$ are shown in the fourth line of Table 1. The fourth and fifth lines compare the results using our default fragmentation algorithm HERPRT with SETPRT (see Section 3) and show very little difference.

Contributions to the event sample from background sources other than the dominant direct W +jet production were studied to determine if they could explain some of the excess at $\ln(L_{rel}^{t170}) > 0$. These additional backgrounds are of two types. First, in the W +jet sample

there is a fraction of non- W events (e.g.: hadrons misidentified as electrons or muons, or real leptons from $b\bar{b}$). As in [1], the number of such events is estimated by extrapolating the number of events which pass the \cancel{E}_T cut but have non-isolated leptons, to the region in which lepton isolation is required. When only the isolation cut is released in the signal sample, no additional event enters. Following this procedure, the signal sample is estimated to contain $0.0^{+0.9}_{-0.0}$ events from this source. The $\ln(L_{rel}^{t170})$ distribution of the non- W events is shown in Figure 12(a) and is similar to the Monte Carlo predicted distribution of VECBOS events.

A second background is WW , WZ events or single Z events with one non-identified decay lepton. The ISAJET Monte Carlo is used to simulate these backgrounds. The WW and WZ backgrounds are normalized with the next-to-leading order computations of the cross section from Ref. [20]. For the Z background the normalization is provided by the measured CDF $Z \rightarrow ee$ cross section [21]. The estimated number of such events in the signal sample is 0.9 ± 0.3 WW events, 0.13 ± 0.05 WZ and $0.14^{+0.06}_{-0.04}$ misidentified Z 's. The $\ln(L_{rel}^{t170})$ distribution of the dominant WW contribution is shown in Figure 12(b). Again, most events are at $\ln(L_{rel}^{t170}) < 0$, as for the QCD single W +jet background. $(21 \pm 9)\%$ of non- W events and $(20 \pm 4)\%$ of WW events are expected at $\ln(L_{rel}^{t170}) > 0$, compared with the $(21.8 \pm 2.4)\%$ for the W +jet background (top line in Table 1).

The probability that the observed excess at positive $\ln(L_{rel}^{t170})$ is consistent with the VECBOS prediction including the effects of non-VECBOS backgrounds and the other systematic errors discussed above is computed as follows. Non-VECBOS events are chosen from a Poisson distribution with the means presented above, and are distributed at positive or negative $\ln(L_{rel}^{t170})$ according to the determined fraction. The remainder of the 14 events are taken to have the $\ln(L_{rel}^{t170}) < 0$ fraction predicted by VECBOS, which is taken to be $(78 \pm 5)\%$. As can be seen from Table 1 this adequately allows for the variations due to changes in the energy scale, Q^2 scale, and the statistical error. The probability is calculated via a Monte Carlo program that includes all the uncertainties mentioned above. The probability is 0.8% to observe ≥ 8 events with $\ln(L_{rel}^{t170}) > 0$ in a sample of 14 events originating from

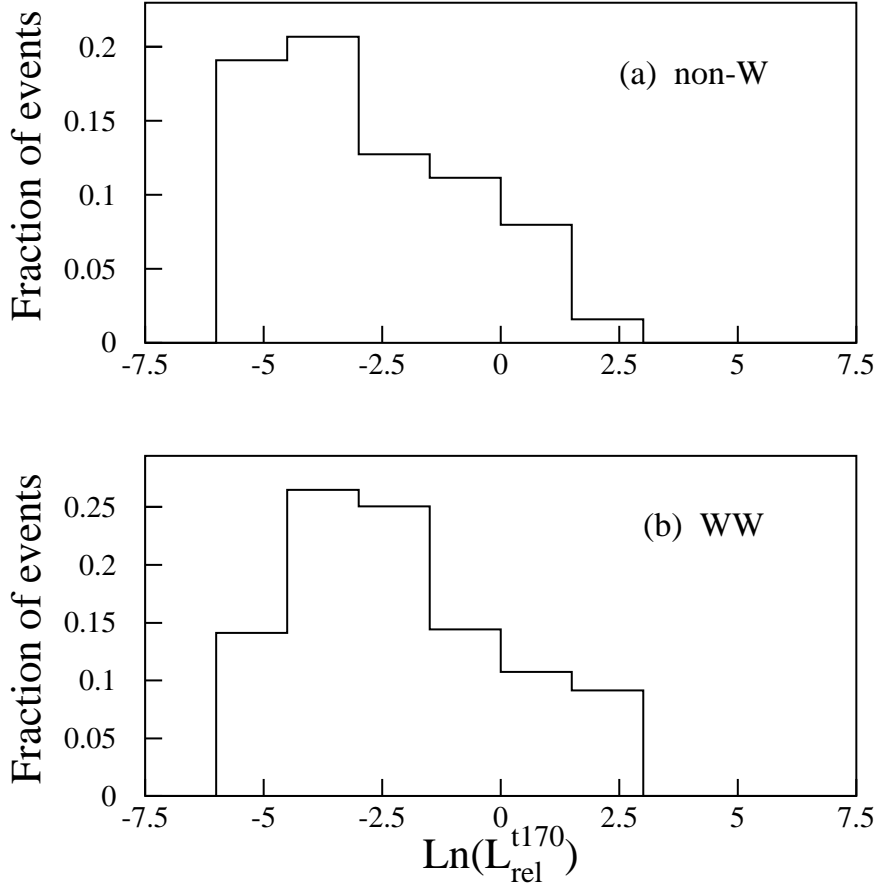


Figure 12: (a) $\text{Ln}(L_{rel}^{t170})$ distribution of non- W background, as derived from the study of a sample of non isolated leptons, with small \cancel{E}_T ; (b) Monte Carlo predicted $\text{Ln}(L_{rel}^{t170})$ distribution of WW events. The distributions are normalized to unit area.

direct W + jets and non- W sources.

We tested whether the results are stable under reasonable variations in the event selection requirements for the signal sample. When we change the requirement on E_{T1} from 20 to 50 GeV, change the cut on $\cos\theta^*$ from 0.7 to either 0.65 or 0.75 or change the jet-jet separation cut from $\Delta R = 0.7$ to 0.6, we get the probabilities for a statistical fluctuation of 0.5%, 1.9%, 0.5% and 0.7% respectively. In the worst case the background fluctuation probability is 1.9%. As an additional test, events were selected with the requirement that the uncorrected missing transverse energy $\cancel{E}_T^{raw} > 20$ GeV, and no cut on the transverse

Figure 13: Distributions of $\ln(L_{rel}^{t170})$ for the control sample. (a) Distributions of VECBOS $W + 3$ jet (dotted histogram) and HERWIG top quark events (solid histogram), normalized to unit area. (b) 35 data events (solid histogram) versus VECBOS (dotted, with statistical errors). VECBOS has been normalized to data in the region $\ln(L_{rel}^{t170}) < 0$.

mass of the W . This is the selection used in Ref. [1]. This sample has about 3 times larger background from fake W events due to misidentified leptons, and the neutrino transverse momentum for real W events is not as well determined. However, the acceptance for W and top quark events is $\simeq 25\%$ larger. This results in a signal sample of 19 events; 11 events are at $\ln(L_{rel}^{t170}) < 0$, 8 at $\ln(L_{rel}^{t170}) > 0$. The probability that ≥ 8 events have $\ln(L_{rel}^{t170}) > 0$ if the events were entirely QCD background is 3.8%.

Figure 13 shows how the 35 events of the control sample are distributed in $\ln(L_{rel}^{t170})$, together with the predictions from VECBOS and HERWIG. The data are well described

by the VECBOS QCD expectation. There is no statistically significant indication for an excess at $\ln(L_{rel}^{t170}) > 0$ (whether this is reasonable is addressed in the next section). For this comparison, $Q^2=M_W^2$ is used as the scale for α_s and structure functions. The use of $Q^2=\langle P_T \rangle^2$ would give a softer spectrum in $\ln(L_{rel}^{t170})$ and the number of predicted QCD events at $\ln(L_{rel}^{t170}) > 0$ would fall by 25%.

5.3 Cross Section Calculation

We assume here that the excess of high jet E_T events in the signal sample results from $t\bar{t}$ production and decay. The most probable numbers of $t\bar{t}$ (N_{top}) and W (N_W) events observed in the signal-enriched and background-enriched samples are estimated using an unbinned maximum likelihood fit to the observed $\ln(L_{rel}^{t170})$ distribution. For this fit, we use the $\ln(L_{rel}^{t170})$ shapes predicted from the HERWIG Monte Carlo program for $t\bar{t}$ events ($M_{top} = 170 \text{ GeV}/c^2$), and from the VECBOS Monte Carlo program for QCD $W + \text{jet}$ events; these predicted shapes are shown in Figure 10(a). The systematic uncertainties on N_{top} and the $t\bar{t}$ production cross section, $\sigma_{t\bar{t}}$, are estimated as a function of M_{top} . The following effects are considered: (1) uncertainty in the jet energy scale, estimated as described in Section 5.2; (2) uncertainty in the Q^2 scale employed by VECBOS to determine the jet E_t spectrum in W events¹, estimated by choosing $Q^2 = \langle P_T \rangle^2$ rather than $Q^2 = M_W^2$; (3) Monte Carlo statistics and uncertainty on the lepton detection efficiency; (4) choice of $t\bar{t}$ Monte Carlo generator (HERWIG, PYTHIA, ISAJET); (5) change of the $\ln(L_{rel})$ shape due to variations of assumed top quark mass in the range $150 < M_{top} < 190 \text{ GeV}/c^2$; (6) the inclusion of non- W , WW , WZ , and misidentified Z contributions in the likelihood fit; (7) uncertainty in the fitting procedure; and (8) uncertainty in data integrated luminosity (this enters only in the calculation of $\sigma_{t\bar{t}}$). The results for the signal sample are summarized in Table 2 for $\sigma_{t\bar{t}}$. The systematic uncertainties on N_{top} are similar to those on $\sigma_{t\bar{t}}$; only the totals are listed in Table 2. The number of $t\bar{t}$ events is found to be $N_{top}=6.4_{-3.2}^{+3.8} \text{ }_{-1.1}^{+1.8}$ and $N_{top} = 0.8_{-0.8}^{+5.3} \text{ }_{-0.8}^{+4.2}$ for the signal and control samples respectively, where the first error is

¹We address the effect of the Q^2 scale on the VECBOS $\ln(L_{rel}^{t170})$ shape only. Absolute rate predictions do not affect the likelihood procedure.

	150 GeV/c ²	170 GeV/c ²	190 GeV/c ²
(1) Jet E _t scale	+21% -19%	+22% -11%	+23% -5%
(2) VECBOS Q ²	+10% -0%	+10% -0%	+10% -0%
(3) MC stat + lepton ϵ	$\pm 10\%$	$\pm 9\%$	$\pm 9\%$
(4) $t\bar{t}$ generator	$\pm 10\%$	$\pm 9\%$	$\pm 10\%$
(5) non- W background	$\pm 2\%$	$\pm 2\%$	$\pm 2\%$
(6) fitting procedure	$\pm 3\%$	$\pm 3\%$	$\pm 3\%$
(7) Luminosity	$\pm 3.6\%$	$\pm 3.6\%$	$\pm 3.6\%$
N _{top} total	+27% -21%	+28% -17%	+24% -16%
$\sigma_{t\bar{t}}$ total	+31% -24%	+33% -23%	+29% -20%

Table 2: Individual systematic errors on $\sigma_{t\bar{t}}$ in the signal sample as a function of M_{top} are listed in rows (1) to (7). Total systematic uncertainties for both N_{top} and $\sigma_{t\bar{t}}$ are summarized in the final two rows.

statistical and the second error is systematic.

The fits indicate more $t\bar{t}$ candidate events in the signal-enriched sample than in the background-enriched sample. The ratio of top quark events in the control sample to top quark events in the signal sample predicted by the Monte Carlo calculation is 1.17 (9.0/7.7). The data fit finds 0.13. However, the statistical significance of the difference from expectation, taking into account the errors, is within 1 σ . The systematic and statistical errors in the determination of N_{top} are significantly larger in the control sample, due to the larger number of QCD W +jet events. From N_{top} , we calculate the corresponding $t\bar{t}$ cross section. This analysis is performed on the signal sample to minimize the systematic effects from the uncertainties in the prediction of the $\ln(L_{rel}^{t170})$ shape for QCD W +jet events. Table 3 shows the total $t\bar{t}$ acceptance, including branching ratios, lepton detection efficiencies and energy scale uncertainty, as a function of the top quark mass, and the results for both N_{top} and $\sigma_{t\bar{t}}$. Figure 14 shows the summed $\ln(L_{rel}^{t170})$ distribution for $t\bar{t}$ and VECBOS corresponding to the Table 3 result (with $M_{top} = 170$ GeV/c²) compared to the observed $\ln(L_{rel}^{t170})$ distribution. The cross section determined from the signal sample is consistent with that found in [1] and, given the large errors, is not inconsistent with the value of $5.7_{-0.6}^{+1.0}$ pb predicted by the theory for a top quark mass of 170 GeV/c² [10].

	$M_{top}=150 \text{ GeV}/c^2$	$M_{top}=170 \text{ GeV}/c^2$	$M_{top}=190 \text{ GeV}/c^2$
$t\bar{t}$ acceptance	$2.7 \pm 0.2\%$	$2.9 \pm 0.2\%$	$3.0 \pm 0.2\%$
N_{top}	$7.9^{+4.6}_{-3.8} \text{ } ^{+2.1}_{-1.6}$	$6.4^{+3.8}_{-3.2} \text{ } ^{+1.8}_{-1.1}$	$5.6^{+3.4}_{-2.8} \text{ } ^{+1.4}_{-0.9}$
$\sigma_{t\bar{t}}$	$15.2^{+8.7}_{-7.3} \text{ } ^{+4.7}_{-3.7} \text{ pb}$	$11.6^{+7.0}_{-5.7} \text{ } ^{+3.8}_{-2.7} \text{ pb}$	$9.6^{+5.9}_{-4.8} \text{ } ^{+2.8}_{-1.9} \text{ pb}$

Table 3: First line: $t\bar{t}$ acceptance for the signal sample. Second and third line: N_{top} and $t\bar{t}$ production cross section $\sigma_{t\bar{t}}$ as a function of M_{top} . The first error on each entry is the data statistical error; the second error on each entry is the sum in quadrature of all systematic errors listed in Table 2.

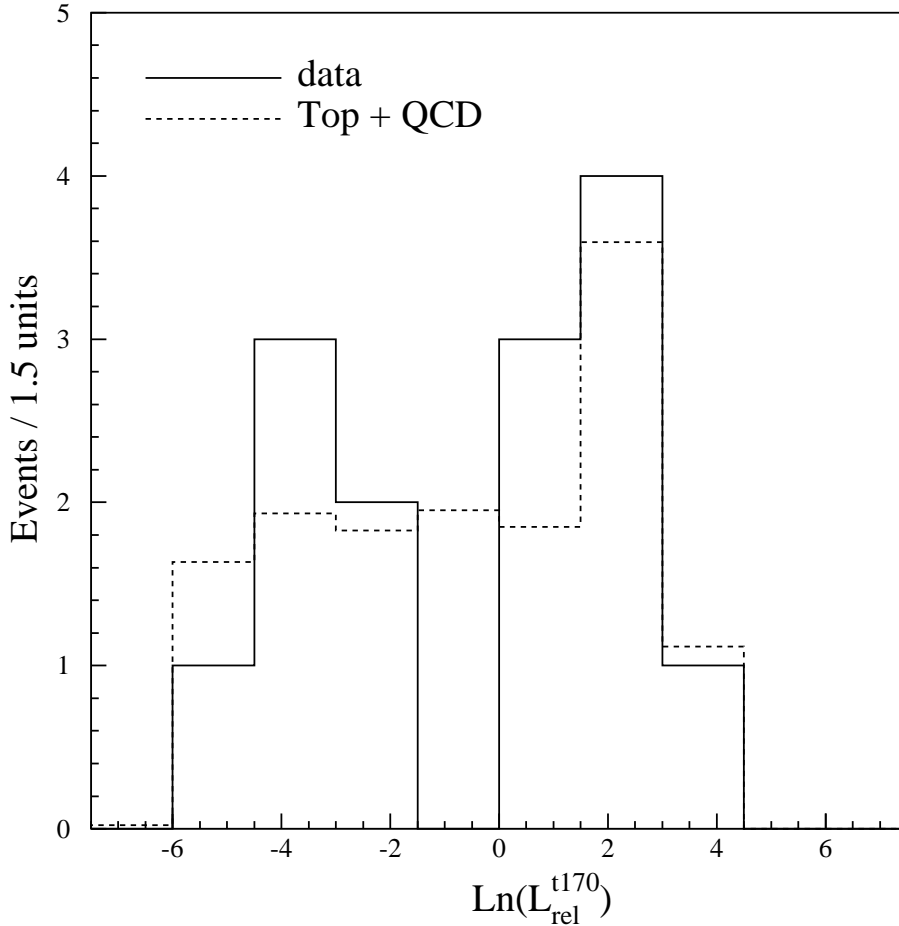


Figure 14: The combined Herwig ($M_{top} = 170 \text{ GeV}/c^2$) + VECBOS $\text{Ln}(L_{rel}^{t170})$ distribution corresponding to the values of N_{top} found (for $M_{top} = 170 \text{ GeV}/c^2$) in Table 3 (dashed) along with the data (solid).

6 Identification of b jets

Each top quark event has two b jets. In contrast, direct W + jet events contain b jets only at the level of a few percent [22]. In this section we use two different methods to identify the b jets in the event (b tagging). In the first method, the Silicon Vertex Detector (SVX) is used to detect B hadrons by reconstruction of secondary vertices separated in the plane transverse to the beam from the primary interaction vertex as a result of the long B hadron lifetime. The algorithm used to reconstruct secondary vertices, “jet-vertexing”, and its performance are discussed extensively in Ref. [1]. For top quark events, the tagging efficiency (i.e the efficiency to tag at least one jet in an event as a b -jet, including detector acceptance) is expected from Monte Carlo to be 24 ± 5 % in the signal sample and 19 ± 5 % in the control sample. The efficiency is larger in the signal sample since more events fall within the fiducial acceptance of the SVX detector. From the number of top quark events derived from the $\ln(L_{rel}^{t170})$ shape analysis above, $1.5_{-0.9}^{+1.0}$ SVX tags are expected from top quark in the signal sample and $0.15_{-0.15}^{+1.30}$ in the control sample. The expected number of SVX tags if no top quark were present in the sample is computed in the same way as in Ref. [1]. The dominant contribution is from $Wb\bar{b}$, $Wc\bar{c}$ and mistags. The background estimate assumes that all the events are background and uses a tag probability for each jet, based on jet E_T , η and track multiplicity, which is derived from a study of a large sample of inclusive jet data [1]. This contribution is found to be 0.47 ± 0.06 events in the signal sample and 0.83 ± 0.11 events in the control sample. Note that these estimates are derived directly from the data and do not rely on Monte Carlo predictions. Adding the other small background contributions to the tags (WW , WZ , Wc , $Z \rightarrow \tau\tau$ and non- W events, see [1]), the total expected number of tags assuming that the data contain no top quark events is $0.58_{-0.09}^{+0.12}$ in the signal sample and 1.1 ± 0.2 in the control sample. In the data, 4 events have a SVX tag in the signal sample (3 in common with the events selected in Ref. [1]) and 1 event is tagged in the control sample. The probability that the tagging rate in the signal sample is consistent with the data being only background is about 0.4 %. On the other hand, the observed numbers of tags are consistent with the mixture of top quark and

background events expected from the kinematic analysis. Including mistags of top quark events and correcting the background estimates for top quark content in the sample, a total of 1.9 ± 1.0 tags is expected in the signal sample and $1.2_{-0.3}^{+1.3}$ in the control sample. These numbers are summarized in Table 4, together with the probability that the observed tag rate is consistent with the respective expectation.

As discussed in Ref. [1], b jets can also be identified by the presence of an electron or muon from semileptonic B decay. For this ‘‘Soft Lepton Tag’’ algorithm (SLT), the top quark tagging efficiencies are expected to be 19 ± 3 % in the signal sample and 13 ± 3 % in the control sample. The expected number of SLT tags, assuming the data do not contain top quark, can be computed in a similar way as for the SVX jet–vertexing tagging algorithm. With all background contributions included, 1.2 ± 0.3 tags are expected in the signal sample and 1.4 ± 0.3 tags in the control sample. In the data, there are 4 SLT tags in

Sample	Obs. tags	Exp. tags backg.	Exp. tags backg. + $t\bar{t}$	Prob. backg.	Prob. backg. + $t\bar{t}$
Signal	4 SVX	$0.58_{-0.09}^{+0.12}$	1.9 ± 1.0	0.4%	16.6%
Control	1 SVX	1.1 ± 0.2	$1.2_{-0.3}^{+1.3}$	66%	81.7%
Signal	4 SLT	1.2 ± 0.3	2.2 ± 0.9	4%	20.7%
Control	1 SLT	1.4 ± 0.3	$1.5_{-0.3}^{+1.0}$	74%	84.7%

Table 4: Summary of b -tagging results in the signal and control samples. Also shown are the probabilities that the observed rate is consistent with background only, or with a mixture of top quark + background.

the signal sample (3 of them in common with Ref [1]) and 1 (also in common with Ref. [1]) in the control sample. Two of the four events tagged by SLT in the signal sample are also tagged by the SVX jet–vertexing algorithm: one of these two is in common with Ref. [1]. In the signal sample there is again an excess of tags over the predicted background.

The observed b -tags in the signal sample have a low probability of being entirely due to a fluctuation in tagging direct W + jet background events. On the other hand, the

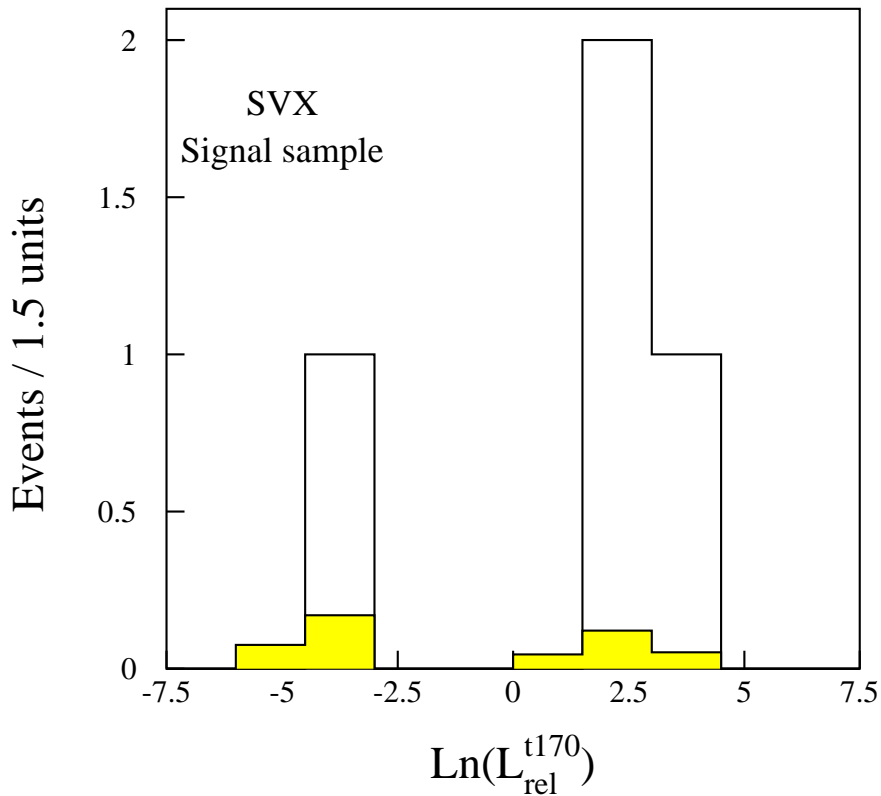


Figure 15: Distribution in $\ln(L_{rel}^{t170})$ of the 4 events of the signal sample tagged by the SVX jet-vertexing algorithm. The expected tags in QCD W +jet events (0.47 in total) are shown as a shaded histogram.

hypothesis that the observed events are a mixture of background and top quark gives a good description of the observed tagging rates for both SVX and SLT tagging methods.

7 Relative Likelihood of b-tagged and four jet Events

The $\ln(L_{rel}^{t170})$ values of the signal sample events are listed in Table 5. One observes that 5 out of 6 b-tagged events are at $\ln(L_{rel}^{t170}) > 0$. The $\ln(L_{rel}^{t170})$ distribution of the 4 SVX tags together with the dominant background from $Wb\bar{b}$, $Wc\bar{c}$ and mistags, estimated from the inclusive jet parametrization, is shown in Figure 15.

HERWIG predicts that about 80% of the top quark events ($M_{top} = 170 \text{ GeV}/c^2$) will exhibit a fourth jet in the CDF detector with transverse energy more than 15 GeV. Due to

Run-Event	$\ln(L_{rel}^{t170})$	SVX	SLT	4th jet	prim. lep.
40758-44414	3.1	•		*	e
43096-47223	3.0	•		*	e
42539-200087	2.2	•	•	*	μ
43351-266423	1.1		•	*	μ
45779-6523	0.7			*	e
42517-44047	-3.5	•	•		μ
44931-59686	-4.3				e
47616-24577	-5.0				e
Run-Event	$\ln(L_{rel}^{t170})$	SVX	SLT	4th jet	prim. lep.
42913-59303	2.2				e
45705-54765	1.6		•	*	e
43276-101844	0.2				μ
45902-240098	-2.2				e
46290-264893	-2.9				e
45801-80320	-3.4				e

Table 5: Summary of the signal sample events. The upper section lists events with at least one jet within the acceptance of the SVX tagging algorithm. The events in the lower section cannot be tagged by the SVX. The fifth column identifies those events which have four or more jets, and the last column identifies the lepton from the W decay as either an electron or muon.

the small value of α_s , the fraction of $W + \geq 4$ jet events expected in a $W + \geq 3$ jet sample is much less. Thus the requirement of a fourth jet should further enrich the sample in top quark events relative to QCD background. The signal sample contains 6 events with four or more jets with $E_T(\text{jet}) > 15$ GeV. These events are indicated with a * in Table 5. They are all at $\ln(L_{rel}^{t170}) > 0$. Figure 16(a) shows their distribution in $\ln(L_{rel}^{t170})$ together with the prediction from the VECBOS $W + 3$ jets + HERPRT fragmentation routine. We recall that in this approach the fourth jet is produced by hard bremsstrahlung from initial and final state partons. Studies using $W + 4$ parton + SETPRT Vecbos simulated events yield similar predictions for background. The normalization chosen for VECBOS in Figure 10(b) predicts 2.3 VECBOS events at $\ln(L_{rel}^{t170}) < 0$ in Figure 16(a), while none is observed. This is compatible at the 10% C.L.. At $\ln(L_{rel}^{t170}) > 0$, 1.0 VECBOS events are predicted compared to the observation of 6 data events. The excess with respect to the QCD prediction at $\ln(L_{rel}^{t170}) > 0$ already observed for $W + \geq 3$ jet events in Figure 10(b), is therefore made relatively more pronounced by the requirement of a fourth jet, showing a positive correlation

between the $\ln(L_{rel}^{t170}) > 0$ and four-jet signature. The four-jet topology and b-tags are also strongly correlated. In three of the 6 four-jet events we find an SVX tag. The distribution in $\ln(L_{rel}^{t170})$ of these 3 events is shown in Figure 16(b). In the absence of top quark, 0.15 background tags are predicted for the dominant direct $W+$ jet production, distributed as shown in the figure.

A similar picture emerges for the SLT tag algorithm, since 3 SLT tags are identified in the $W + 4$ jet sample. In conclusion, 6 out of the 8 events at $\ln(L_{rel}^{t170}) > 0$ of Fig. 10(b) have at least one additional jet, and 5 of them are b-tagged. This is very unlikely to be due to background, and is more consistent with $t\bar{t}$ events.

Using the methods described in Ref. [1] we have computed the top quark mass for the subset of events of the signal and control sample with exclusively four jets, by requiring $E_{T4} > 15$ GeV and $E_{T5} < 10$ GeV. Four events fulfill this requirement: three belong to the signal sample and one to the control sample. The three of the signal sample (all at $\ln(L_{rel}^{t170}) > 0$) are in common with the $W+$ jet event sample of Ref. [1]) and are among the 7 tagged events used in [1] for the derivation of the top quark mass.

The masses of these 4 events are in the range 161 ± 11 GeV/ c^2 to 172 ± 11 GeV/ c^2 , lower on average but consistent with the result of $M_{top} = 174 \pm 10^{+13}_{-12}$ reported in Ref. [1]. We have compared their mass distribution with the distributions expected for $t\bar{t}$ and direct $W+4$ jet events. The expected distributions for top quark and for direct $W+$ jet production are appreciably different. Within the very poor statistics, the distribution of the data events, shown in Figure 17, favours the $t\bar{t}$ hypothesis over QCD.

8 Conclusions

The kinematics of a sample of 49 $W+ \geq 3$ jet events was compared with the theoretical expectations for direct $W+$ jet production and $t\bar{t}$ quark pair production. It is determined whether a given $W+ \geq 3$ jet event fits better the expectations of direct $W+$ jet production as predicted by the VECBOS QCD Monte Carlo or top quark as predicted by the HERWIG Monte Carlo. The VECBOS predictions for $W+ \geq 2$ central jets and $Z+ \geq 3$ jet production

agree well with the observed data. A subsample of $W + \geq 3$ jet events (“control sample”) that should be enriched in direct W production events relative to top quark has been defined. VECBOS also gives a good description of the observed jet E_T distributions for this sample. A separate subsample (“signal sample”) is defined with the requirement that the three leading jets be central. It should be enriched in $t\bar{t}$ events relative to direct $W +$ jet events which form the main background. This signal sample contains 14 events. The jet E_T distributions for these events are unusually hard and not well described by the expectations from QCD and other backgrounds. By means of a suitable variable, $\ln(L_{rel}^{t170})$, events that are kinematically more top quark-like can be selected as those events with $\ln(L_{rel}^{t170}) > 0$. We observe 8 such events, while we expect 1.7 from non-top quark processes. From a statistical analysis, which takes into account the systematic errors, we have derived a probability of 0.8% for this excess to be due entirely to background fluctuations. The analysis was repeated for a number of different selection cuts defining the signal sample, and in the worst case a probability for such a fluctuation as large as 1.9% was found. A two component fit to the data that includes contributions from a 170 GeV/ c^2 mass top quark and from QCD and other backgrounds gives a good description of the observed jet E_T distributions, and yields a $t\bar{t}$ production cross section of $11.6_{-5.7}^{+7.0} +3.2_{-2.0}$ pb, consistent with the findings of Ref. [1]. A similar two component fit to the background enriched control sample yields a cross section which is 1 sigma below this value, and statistically consistent with zero.

With a secondary vertex b -tag algorithm (SVX) we find evidence for bottom quark decay in four of the 14 events in the signal enriched sample. If the 14 events contained no contribution from top quark, only 0.58 events with such a secondary vertex b -tag are expected. The probability for four events to be tagged due to a statistical fluctuation is 0.4%. Similarly, this same event sample of 14 events contains 4 soft lepton tags (SLT) with an expected background of 1.2 events. The probability for four events to be tagged due to a statistical fluctuation is about 4% in this case.

Additional information on the nature of the events at $\ln(L_{rel}^{t170}) > 0$ was obtained from their large probability of containing a fourth jet. In the signal sample, out of a total of 8

events at $\ln(L_{rel}^{t170}) > 0$, there are 6 four-jet events and 5 of them are b-tagged. Assuming that b-tags are indicative of $t\bar{t}$ pairs, one can argue that the events at $\ln(L_{rel}^{t170}) > 0$ show an increased top quark purity when the kinematic cuts are made more stringent (a 4th jet is required). We note that 5 out of 6 b-tagged events of the signal sample listed in Table 5 are in common with the b-tagged sample of Ref. [1]. This shows that, although the primary event sample selected in this analysis overlaps only in part with the W +jet sample of Ref. [1] (25 events in common), the two analysis strategies have isolated the same physics process. The evidence for top quark reported in [1] was derived only on the basis of the observed excess of di-leptons and b-tags. The observation of a top quark-like component in the $\ln(L_{rel}^{170})$ distribution reported here provides additional evidence, independent of that provided by the counting experiments reported in Ref. [1], that our data contains a fraction of events more consistent with the decays of top quarks of mass around $170 \text{ GeV}/c^2$ than with the W +jet background.

9 Acknowledgments

We thank the Fermilab staff and the technical staffs of the participating institutions for their vital contributions. We also thank Walter Giele for advice and many helpful suggestions regarding W +jets and the VECBOS Monte Carlo program. This work is supported by the U.S. Department of Energy and the National Science Foundation; the Italian Istituto Nazionale di Fisica Nucleare; the Ministry of Science, Culture, and Education of Japan; the Natural Sciences and Engineering Council of Canada; the A. P. Sloan Foundation; and the Alexander von Humboldt-Stiftung.

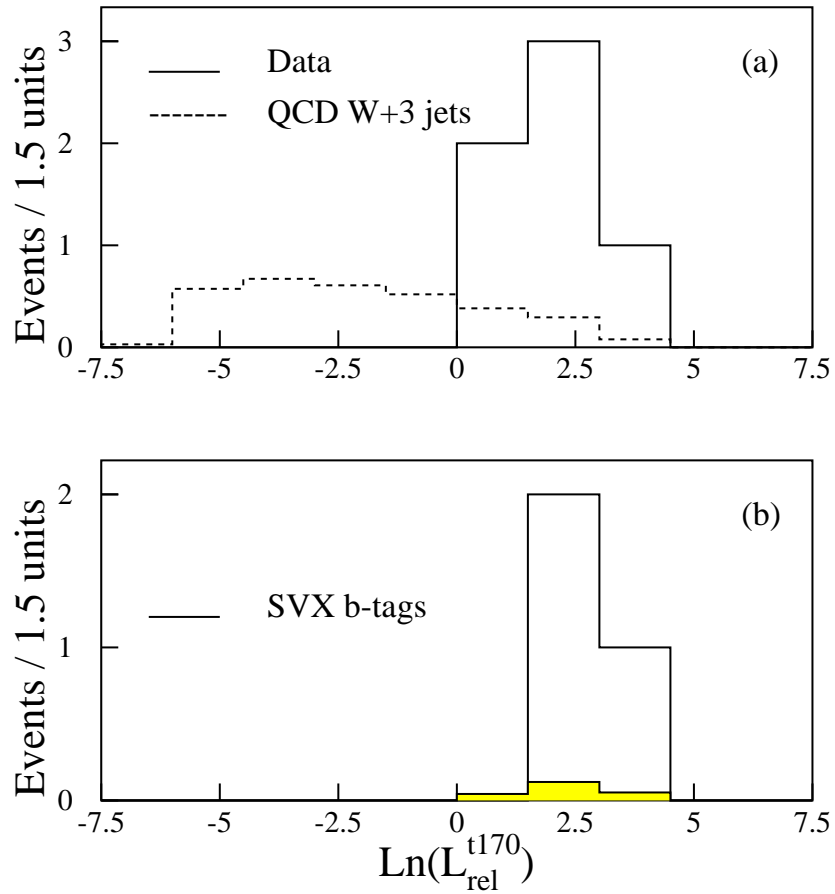


Figure 16: Distribution in $\ln(L_{rel}^{t170})$ of $W+ \geq 4$ jet events. (a) data with VECBOS prediction. (b) events with a SVX secondary vertex and prediction (shaded) based on the observed jets in the events.

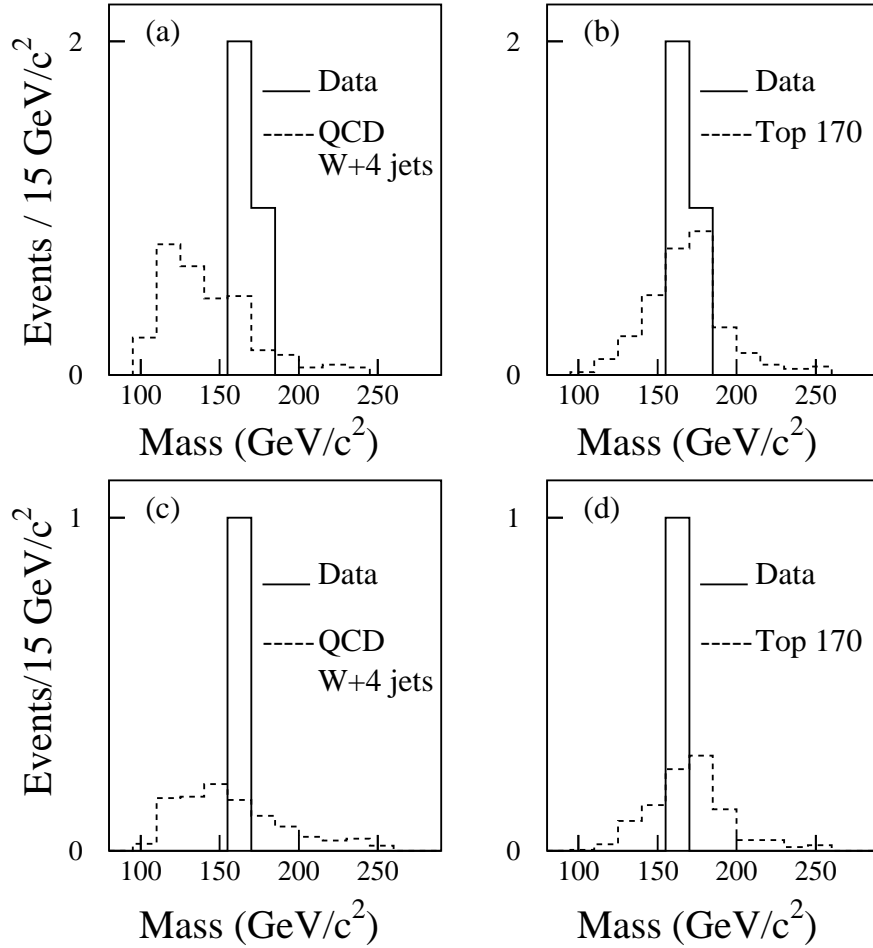


Figure 17: Distribution of the expected mass for VECBOS Monte Carlo events, analyzed as they were $t\bar{t}$ events (dashed histogram) (a) for the signal sample and (c) for the control sample cuts. Distribution of the preferred mass for $t\bar{t}$ ($M_{top} = 170 \text{ GeV}/c^2$) Monte Carlo events, analyzed as $t\bar{t}$ (b) for the signal sample and (d) for the control sample cuts. The 4 events which allow the mass reconstruction are shown as solid histograms.

References

- [1] F. Abe *et al.*, Phys. Rev. Lett. **73**, 225 (1994), and Phys. Rev. D **50**, 2966 (1994).
- [2] S. Abachi *et al.*, Phys. Rev. Lett. **72**, 2138 (1994);
“Search for High Mass Top Quark Production in $p\bar{p}$ collisions at $\sqrt{s}=1.8$ TeV”,
FERMILAB-PUB-94/354-E, submitted to Phys. Rev. Lett.
- [3] B. Pietrzyk for the LEP collaborations, preprint LAPP-EXP-97.07 (May 1994).
- [4] F. Abe *et al.*, Nucl. Instrum. Methods **A271**, 387 (1988).
- [5] D. Amidei *et al.*, Nucl. Instrum. Methods **A350**, 73 (1994).
- [6] Pseudorapidity, η , is defined as $\eta=-\ln(\tan(\theta/2))$ where θ is the polar angle in spherical coordinates, measured from the proton beam axis assuming a z-vertex position of zero.
- [7] F. Abe *et al.*, Phys. Rev. D **45**, 1448 (1992).
- [8] F. Abe *et al.*, Phys. Rev. D **47**, 4857 (1993).
- [9] S. Leone, Ph.D. Thesis, Pisa 1994, INFN PI/AE 94/007.
- [10] E. Laenen, J. Smith and W.L. van Neerven, Phys. Lett. **321B**, 254 (1994).
- [11] F. Paige and S. D. Protopopescu, BNL Report No. 38034, 1986 (unpublished).
- [12] G. Marchesini and B.R. Webber, Nucl. Phys. **B310**, 461 (1988);
G. Marchesini *et al.*, Comput. Phys. Comm. **67**, 465 (1992).
- [13] F.A. Berends, W.T. Giele, H. Kuif, B. Tausk, Nucl. Phys. **B357**, 32 (1991);
W.Giele, Ph.D. Thesis, unpublished.
- [14] R. Field and R. Feynmann, Nucl. Phys. **B136**, 1 (1978).
- [15] J. Benlloch, CDF Collaboration, Proceedings of the 1992 DPF Meeting, 10–14 Nov.,
1992 Batavia, Il, ed. C. H. Albright *et al.*, World Scientific, (1993) p. 1091.

- [16] K. Kondo, J. Phys. Soc. Japn. **57**, 4126 (1988);
K. Kondo, J. Phys. Soc. Japn. **60**, 836 (1991).
- [17] M.Cobal, H. Grassmann and S. Leone, Il Nuovo Cimento, **107A**, 75 (1994);
M. Cobal, Ph.D. Thesis, Pisa 1994, INFN PI/AE 94/004.
- [18] F.Abe *et al.*, Phys. Rev. Lett., **70**, 4042 (1993).
- [19] J.Alitti *et al.*, Phys. Lett. **268B**, 145 (1992).
- [20] For the WW production cross section we used the value 9.5 pb, see:
J. Ohnemus *et al.*, Phys. Rev. D **44**, 1403 (1991);
S. Frixione, Nucl. Phys. **B410**, 280 (1993);
J. Ohnemus and J.F. Owens, Phys. Rev. D **43**, 3626 (1991);
J. Ohnemus, Phys. Rev. D **44**, 3477 (1991);
S. Frixione, P. Nason and G. Ridolfi, Nucl. Phys. **B383**, 3 (1992).
- [21] F. Abe *et al.*, Phys. Rev. D **44**, 29 (1991).
- [22] M.L. Mangano, Nucl. Phys. **B405**, 536 (1993).

